

**PARTICLE SWARM OPTIMIZATION BASED  
INVERTER IMPEDANCE CONTROL TO  
PERFORM HARMONIC SHARING IN  
ISLANDED MICROGRID**

**LAILATUL NIZA BINTI MUHAMMAD**

**RESEARCH VOTE NO:  
RDU1703221**

**UMP**

**Fakulti Kejuruteraan Elektrik dan Elektronik  
Universiti Malaysia Pahang**

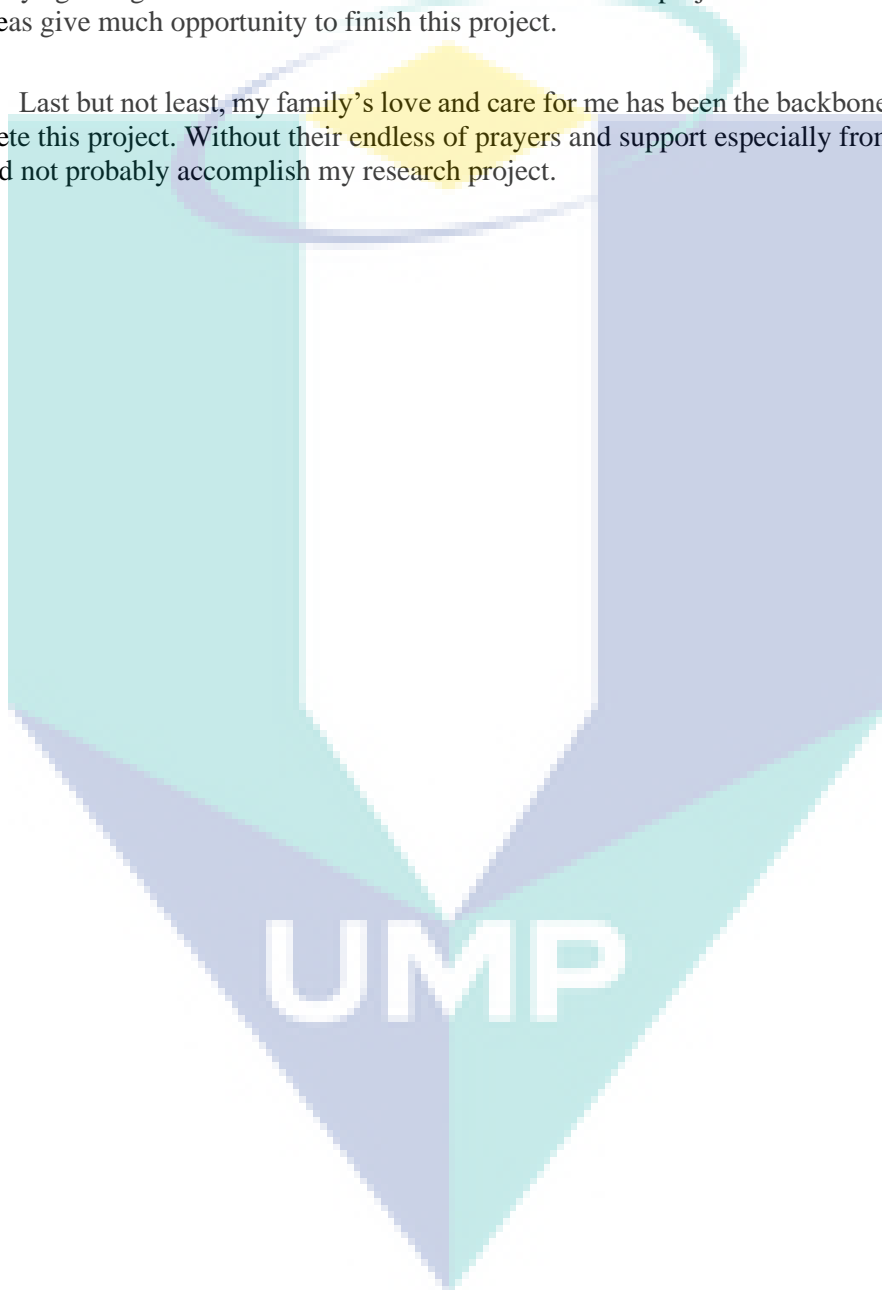
**2019**

## ACKNOWLEDGEMENTS

Firstly, I would like to thank my FYP student, CHRISTOPHER NGADI ANAK JULIUS for his ambitious together to complete this project research.

Secondly, I would also like to convey my sincere appreciation to Dr. Hamdan bin Daniyal for always guiding me whenever I face difficulties in this the project research. His consultation and ideas give much opportunity to finish this project.

Last but not least, my family's love and care for me has been the backbone throughout to complete this project. Without their endless of prayers and support especially from my husband, I would not probably accomplish my research project.



## ABSTRACT

Distributed generation (DG) is referred as an integration of different kinds of renewable energy sources used to generate electricity at or near the location where it will be utilized, such as solar panels, combined heat and power and others. Voltage source inverters located between the DG and utility grid plays an important part in injecting clean and reliable power into the grid. Several control issues arises from the grid integration of PV based system such as grid stability, power quality control, loads sharing and others. A power quality index known as total harmonics distortion (THD) is an indicator used to measure the harmonics content in a distorted waveform. The THD of voltage and current for grid connected system should be below 5% as mentioned in IEEE 519-2014 Standard. This project focuses on the power quality control of harmonics in grid current due to nonlinear load in the system. A comparative study between current control techniques namely Hysteresis current controller, Proportional-Integral (PI) controller and combination of Proportional-Integral (PI) with Hysteresis current controller is conducted to control the harmonics distortion in grid current. The impact of nonlinear load on grid current is analyzed by measuring the performance of THD<sub>i</sub> level in MATLAB™ Simulink software environment.

Key researcher:

THDi, harmonics, hysteresis current control, power quality, Proportional-Integral, Renewable energy sources

The logo for Universiti Malaysia Perlis (UMP) is a large, stylized letter 'V' shape. The left side of the 'V' is light blue, the right side is light green, and the bottom point is a darker blue. The letters 'UMP' are written in white, bold, sans-serif font across the center of the 'V'.

Email: [lailatul@ump.edu.my](mailto:lailatul@ump.edu.my)

Tel no: 0122709382

Vote No: RDU1703221

## ABSTRAK

Generasi pengagihan disebut sebagai gabungan pelbagai sumber tenaga boleh diperbaharui yang digunakan untuk menjana tenaga elektrik pada atau berhampiran di mana ia akan digunakan, seperti panel solar, gabungan haba dan kuasa serta lain-lain. Penyongsang sumber voltan terletak di antara generasi pengagihan dan grid utiliti memainkan peranan penting dalam menyuntik tenaga bersih dan efektif ke dalam grid. Beberapa isu kawalan timbul daripada integrasi sistem grid-PV iaitu seperti kestabilan grid, kawalan kualiti kuasa, beban perkongsian dan lain-lain. Satu indeks kualiti kuasa dikenali sebagai jumlah harmonik herotan merupakan petunjuk yang digunakan untuk mengukur kandungan harmonik dalam bentuk gelombang voltan dan arus. Kandungan harmonik dalam arus grid sepatutnya berada pada tahap kurang daripada 5% seperti yang disebut dalam *IEEE 519-2014 Standard*. Projek ini memberi tumpuan kepada kawalan kualiti kuasa harmonik dalam arus grid disebabkan oleh beban yang tidak seimbang dalam sistem. Satu kajian perbandingan antara teknik kawalan arus iaitu *Hysteresis current controller*, *Proportional-Integral (PI) controller* dan gabungan *Proportional-Integral (PI)* dengan *Hysteresis current controller* telah dijalankan untuk mengimbangi herotan harmonik dalam arus grid. Kesan beban yang tidak seimbang pada arus grid dianalisis dengan mengukur tahap kandungan harmonik melalui perisian MATLAB™ Simulink.

The logo of UMPA (Universiti Malaysia Perlis) is a large, stylized letter 'V' shape. The left side of the 'V' is light blue, the right side is a darker blue, and the bottom point is a teal color. The letters 'UMPA' are written in white, bold, sans-serif font across the center of the 'V' shape.

UMPA

## TABLE OF CONTENT

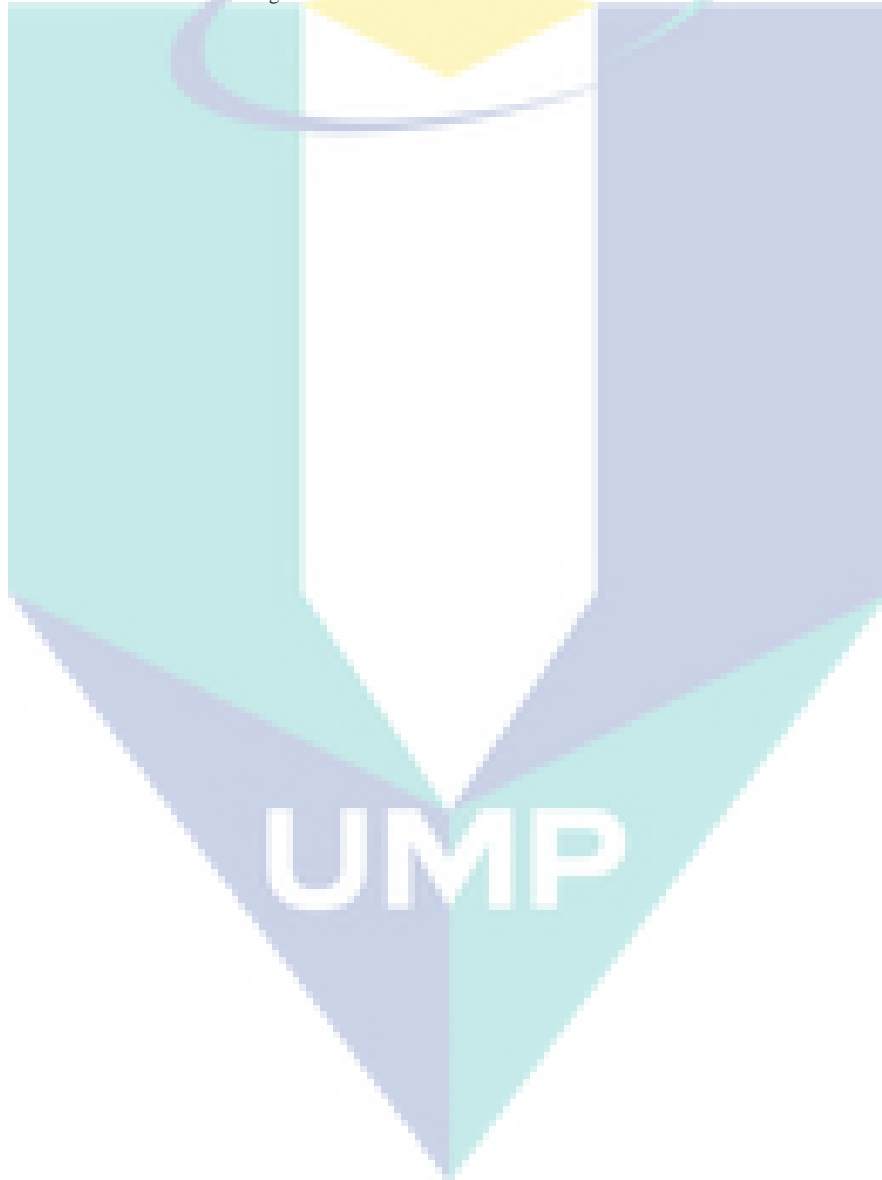
<b>TITLE PAGE</b>	
<b>ACKNOWLEDGEMENTS</b>	<b>ii</b>
<b>ABSTRAK</b>	<b>iv</b>
<b>ABSTRACT</b>	<b>iii</b>
<b>TABLE OF CONTENT</b>	<b>v</b>
<b>LIST OF TABLES</b>	<b>viii</b>
<b>LIST OF FIGURES</b>	<b>ix</b>
<b>LIST OF ABBREVIATIONS</b>	<b>xi</b>
<b>CHAPTER 1 INTRODUCTION</b>	<b>1</b>
1.1 Project Background	1
1.2 Problem Statements	3
1.3 Objectives	3
1.4 Project Scope	4
1.5 Thesis Outline	4
<b>CHAPTER 2 LITERATURE REVIEW</b>	<b>5</b>
2.1 Introduction to Microgrid & DG	5
2.2 Inverter Classification	7
2.2.1 Voltage Source Inverter	7
2.2.1.1 Single Phase Inverter	9
2.2.1.2 Three Phase Inverter	10
2.3 Pulse Width Modulation Technique	11
2.3.1 Single Pulse Width Modulation	11
2.3.2 Multiple Pulse Width Modulation	12

2.3.3	Sinusoidal Pulse Width Modulation	13
2.4	Grid-Tie Inverter System	14
2.4.1	Classification of Grid Synchronization Method	15
2.5	Control System	16
2.5.1	Open Loop System	16
2.5.2	Closed Loop System	17
2.6	Classification of Current Controllers	18
2.6.1	Hysteresis Controller	20
2.6.2	Proportional Integral	21
<b>CHAPTER 3 METHODOLOGY</b>		<b>23</b>
3.1	Flowchart of Project	23
3.2	Block Diagram of Overall Project	26
3.2.1	Simulation Parameters	28
3.3	System Design	29
3.3.1	Single Phase Inverter System Design	29
3.3.2	PWM Generator	30
3.3.3	LC Filter Selection	30
3.4	Non-Linear Load	32
3.5	Grid Modelling	32
3.6	Controller Design	34
3.6.1	Hysteresis Current Controller Modelling	34
3.6.2	PI Controller Modelling	36
3.6.3	PI with Hysteresis Current Controller Modelling	37
3.7	Performance Measures	39
3.7.1	Total Current Harmonics Distortion (THD <sub>i</sub> )	39

<b>CHAPTER 4 RESULTS &amp; DISCUSSIONS</b>	<b>40</b>
4.1 Single Phase Full Bridge Inverter with SPWM	40
4.2 Single Phase VSI under Nonlinear Load (with LC Filter)	42
4.3 Single Phase VSI Grid-Connected Under Nonlinear Load (Without Current Controller)	44
4.4 Single Phase VSI Grid-Connected Inverter with Current Control	46
4.4.1 Single Phase VSI Grid-Connected Inverter with Hysteresis Current Controller	46
4.4.2 Single Phase VSI Grid-Connected Inverter with PI Controller	48
4.4.3 Single Phase VSI Grid-Connected Inverter with PI with Hysteresis Current Controller	50
4.5 Table of Comparison between Current Controllers	52
4.5.1 Harmonics Spectrum of $I_{grid}$	54
4.5.2 $THD_i$ Comparison of Without and With Current Controllers	55
<b>CHAPTER 5 CONCLUSION</b>	<b>56</b>
5.1 Summary of Project	56
5.2 Suggestions/Recommendations for Future Work	56
<b>REFERENCES</b>	<b>58</b>

## LIST OF TABLES

Table 1-1 Comparison between VSI and CSI (28)	8
Table 2-2 Comparison of current control methods	19
Table 3-1 Simulation parameters of circuit	28
Table 4-1 Switching states for single phase VSI	40
Table 4-2 Comparison of $V_{inv}$ , $I_{grid}$ , and $THD_i$ of $I_{grid}$	52
Table 4-3 $THD_i$ values of $I_{grid}$ without and with current controllers	55





## LIST OF FIGURES

Figure 1.1 Average annual increase of renewable electricity generation from 2012-2040 [1]	1
Figure 1.2 Grid-connected inverter structure	2
Figure 1.3 IEEE 519-2014 Standards [23]	2
Figure 2.1 Microgrid concept [27]	5
Figure 2.2 Power electronic based converter classification [28]	7
Figure 2.3 Self-commutated VSI inverter [28]	8
Figure 2.4 Single phase full-bridge inverter IGBT [15]	9
Figure 2.5 Three-phase inverter with LC filter [4]	10
Figure 2.6 Single PWM output [15]	11
Figure 2.7 Multiple PWM output [15]	12
Figure 2.8 Sinusoidal PWM output [16]	13
Figure 2.9 Single-phase VSI grid tie inverter under nonlinear load schematic diagram [2]	14
Figure 2.10 Grid synchronization methods for single phase and three phase system [20]	15
Figure 2.11 LCL-based grid-connected inverter [21]	16
Figure 2.12 PI with hysteresis in single phase boost inverter [11]	17
Figure 2.13 Classification of linear and non-linear current controllers for single phase VSI [1]	18
Figure 2.14 Hysteresis controller block diagram [5]	20
Figure 2.15 Switching pattern of hysteresis control [5]	20
Figure 2.16 Proportional-Integral controller block diagram [18]	21
Figure 2.17 Single-phase grid connected inverter with PI controller structure [25]	21
Figure 3.1 Stage-by-stage development of project	23
Figure 3.2 Overall flowchart of project	25
Figure 3.3 Block diagram of project	26
Figure 3.4 Single phase PMW-VSI Simulink block	29
Figure 3.5 PWM generator for single phase inverter simulation block	30
Figure 3.6 Single phase inverter with LC filter simulation block	31
Figure 3.7 Diode rectifier (R-C load) as nonlinear load	32
Figure 3.8 Input voltage of grid (left) and reference voltage from grid (right) configuration tab	33

Figure 3.9 Single phase PWM-VSI connected to grid simulation block	33
Figure 3.10 Hysteresis controller simulation block	35
Figure 3.11 PI controller simulation block	36
Figure 3.12 $I_{ref}$ generation for PI with hysteresis current controller	37
Figure 3.13 PI with hysteresis current controller simulation block	38
Figure 4.1 Reference signal as sine wave and carrier signal as sawtooth generator	40
Figure 4.2 Zoom-in view of reference signal carrier signal	41
Figure 4.3 Switching states of IGBTs	41
Figure 4.4 Input and output voltage of inverter, $V_{inv}$	42
Figure 4.5 Output current of inverter, $I_{inv}$	42
Figure 4.6 Output load current, $I_{load}$	43
Figure 4.7 Harmonics spectrum of $I_{load}$	43
Figure 4.8 Input and output voltage of inverter, $V_{inv}$ without current control	44
Figure 4.9 Output current inverter, $I_{inv}$ without current control	44
Figure 4.10 Output grid current, $I_{grid}$ without current control	45
Figure 4.11 THD <sub>i</sub> of grid current, $I_{grid}$ without current controllers	45
Figure 4.12 Input and output voltage inverter, $V_{inv}$ with hysteresis current controller	46
Figure 4.13 Output current inverter, $I_{inv}$ with hysteresis current controller	46
Figure 4.14 Output grid current, $I_{grid}$ with hysteresis current controller	47
Figure 4.15 THD <sub>i</sub> of grid current, $I_{grid}$ for hysteresis current control	47
Figure 4.16 Input and output voltage inverter, $V_{inv}$ with PI controller	48
Figure 4.17 Output current inverter, $I_{inv}$ with PI controller	48
Figure 4.18 Output grid current, $I_{grid}$ with PI controller	49
Figure 4.19 THD <sub>i</sub> of grid current, $I_{grid}$ for PI controller	49
Figure 4.20 Input and output voltage inverter, $V_{inv}$ of PI with hysteresis current controller	50
Figure 4.21 Output current inverter, $I_{inv}$ of PI with hysteresis current controller	50
Figure 4.22 Output grid current, $I_{grid}$ of PI with Hysteresis current controller	51
Figure 4.23 THD <sub>i</sub> of grid current, $I_{grid}$ for PI with Hysteresis Current Controller	51
Figure 4.24 Harmonics spectrum of $I_{grid}$ given by all three current controllers	54
Figure 4.25 Current THD% of without and with current controllers	55

## LIST OF ABBREVIATIONS

THD <sub>i</sub>	Total Current Harmonic Distortion
PI	Proportional-Integral
PWM	Pulse Width Modulation
SPWM	Sinusoidal Pulse Width Modulation
DG	Distributed Generation
RES	Renewable Energy Sources
VSI	Voltage Source Inverter
$K_p$	Proportional Gain
$K_i$	Integral Gain
HB	Hysteresis Band
PLL	Phase Locked Loop
PCC	Point of Common Coupling

The logo for UIMP (University of Malakka) is a large, downward-pointing arrow shape. It is composed of four triangular sections meeting at a central point. The top-left and bottom-right sections are light blue, while the top-right and bottom-left sections are a slightly darker shade of blue. The letters 'UIMP' are printed in a bold, white, sans-serif font across the center of the arrow's shaft.

UIMP

# CHAPTER 1

## INTRODUCTION

### 1.1 Project Background

Nowadays, variety of renewable energy applications which includes solar energy, wind energy, hydro, geothermal, tidal and wave energy had been implemented in distributed generation system. Due to the rapid development of renewable energy technologies, it has steered to the production of low cost renewable power generation. RES are highly demand due to its many advantages such as high sustainability, economic profits and able to provide clean energy which makes it environmental-friendly. Referring to Figure 1.1, solar has been targeted as the fastest growing form of renewable energy with an expected average net increase of 8.3% per year, followed by wind and geothermal energy [1]. Some of the common solar applications include solar PV power plants, PV lighting system, residential PV and others.

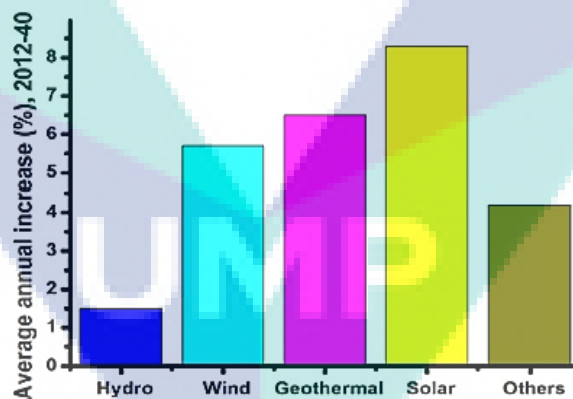


Figure 1.1 Average annual increase of renewable electricity generation from 2012-2040 [1]

The integration of renewable energy based power plant into distributed system leads to the rise of power electronic converters' usage. The power generated by renewable energy sources based distributed generation is transformed by converter into the form of power that is reconcilable with distributed grid as shown in Figure 1.2. However, the power exchange between DG and the grid raises several control issues. One of the

challenging issues is power quality control. The presence of harmonics due to combination between VSI and DC with grid or nonlinear loads causes voltage and current signals to be distorted and injected into the grid by DG inverter. Besides that, large transients due to unsynchronous problem between grid tied converter and the utility grid might cause severe damage to the system. Environmental factors such as solar irradiance, temperature and wind speed affects inconsistent power output to be delivered into DG system by renewable energy sources.

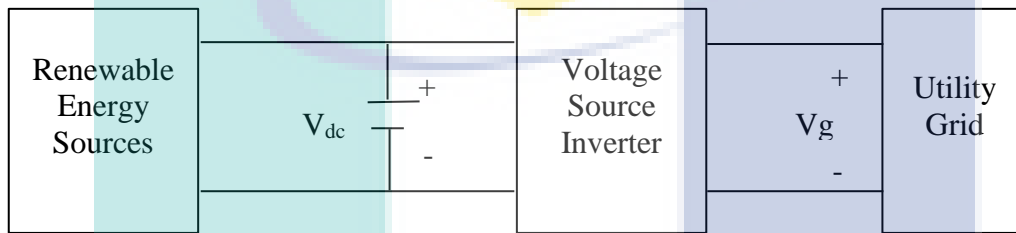


Figure 1.2 Grid-connected inverter structure

Due to the control issues as mentioned in above paragraph, various current control strategies had been proposed by researchers to compensate harmonics content in output waveform of inverter. The most significant current control strategies include PI control, predictive current controller, state feedback controller, ramp-time current controller and hysteresis controller. A power quality index known as total harmonics distortion (THD) is used to measure the harmonics content in the distorted waveform. The THD level of current injected to the grid should be lower than 5% as stated by IEEE 519-2014 Standard [23] in Figure 1.3.

Table 2—Current distortion limits for systems rated 120 V through 69 kV

Maximum harmonic current distortion in percent of $I_L$						
Individual harmonic order (odd harmonics) <sup>a, b</sup>						
$I_{sc}/I_L$	$3 \leq h < 11$	$11 \leq h < 17$	$17 \leq h < 23$	$23 \leq h < 35$	$35 \leq h \leq 50$	TDD
<20 <sup>c</sup>	4.0	2.0	1.5	0.6	0.3	5.0
20 < 50	7.0	3.5	2.5	1.0	0.5	8.0
50 < 100	10.0	4.5	4.0	1.5	0.7	12.0
100 < 1000	12.0	5.5	5.0	2.0	1.0	15.0
> 1000	15.0	7.0	6.0	2.5	1.4	20.0

Figure 1.3 IEEE 519-2014 Standards [23]

## 1.2 Problem Statements

In order to overcome the power quality control issue caused by nonlinear loads in grid-tied inverter system, we had proposed the solution of reducing harmonics content in voltage and current output waveform by implementing two current controllers namely Proportional-Integral (PI) controller and hysteresis controller in the project. In general, PI controller consists of two control gains;  $K_p$  to reduce error and  $K_i$  to achieve steady state. For hysteresis controller, it constantly turns the output ON/OFF based on setpoint value.

Hence, the comparative study between hysteresis current controller, Proportional Integral (PI) controller and combination of PI with hysteresis current controller are analysed in the project. All of these current controllers are designed and simulated in single phase grid-connected inverter system to compensate total current harmonics distortion ( $THD_i$ ) problem in grid current due to nonlinear load using MATLAB™ Simulink.

## 1.3 Objectives

The main purpose of this project is to meet the following objectives :

- i. To design single phase inverter under non-linear load condition in MATLAB™ Simulink.
- ii. To design hysteresis current controller, PI controller and combination of PI with hysteresis current controller in single phase grid-connected inverter system.
- iii. To analyse the performance of the controller by conducting comparative study between hysteresis current controller, PI controller and combination of PI with hysteresis current controller by measuring the performance of  $THD_i$  level.

## 1.4 Project Scope

The scopes of the project include:

- i. Design Proportional Integral (PI) controller, hysteresis controller and combination of PI with hysteresis current controller in grid-connected inverter system using MATLAB™ Simulink.
- ii. Analyse and compare total current harmonics distortion (THD<sub>i</sub>) level and output current and voltage waveform shape between PI controller, hysteresis current controller and combination of PI with hysteresis current controller.
- iii. The limitations of single phase grid-connected inverter.

## 1.5 Thesis Outline

The focus of this thesis is the performance of controllers in mitigating harmonics in single-phase grid connected inverter under nonlinear condition. The organization of this thesis is as below.

Chapter 1 presents the project background, problem statements, objectives and project scope of this research.

Chapter 2 explains the existing system done by previous researchers regarding grid-connected inverter with current controllers such as PI controller, hysteresis controller and others.

Chapter 3 reveals the methodology of the project. Simulation system design, controllers' development and performance measures are further explained in this chapter.

Chapter 4 discuss on the results obtained at the end of project. This include the THD<sub>i</sub> level of grid current, as well as different order of harmonics spectrum.

Chapter 5 summarise the overall of project and suggestions for future work.

## CHAPTER 2

### LITERATURE REVIEW

#### 2.1 Introduction to Microgrid & DG

The term called ‘microgrid’ is belonged to a part of distributed resource units and loads to provide connection to/from the main grid by ensuring reliable service during disturbances which can operate in standalone or grid-connected mode [27]. The main role of microgrid is to regulate distributed generation units in an optimum amount without having complex network. Among the major components of microgrid include a point of common coupling (PCC) and local information used to control DG systematically to assure dependable system of operation. In order to ensure the regulation of voltage, frequency and power flow are controllable, several equipments are needed such as DG units, energy storage system, loads and protection scheme as shown in Figure 2.1. Microgrid can be classified into three types; AC microgrid, DC microgrid and hybrid microgrid.

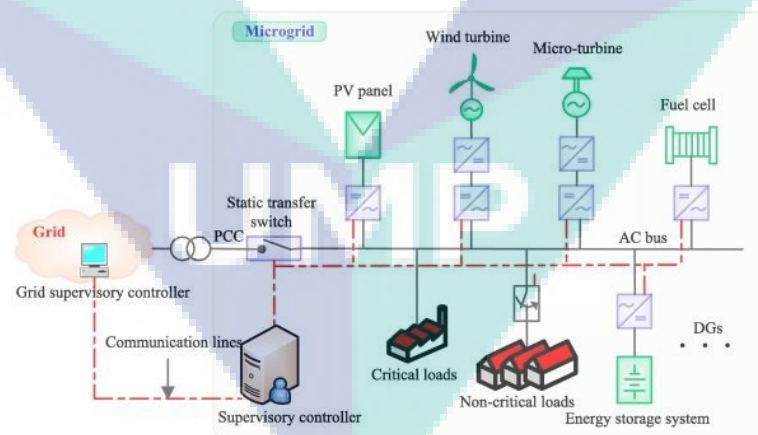


Figure 2.1 Microgrid concept [27]

Distributed generation is described as the combination of variety renewable energy sources to generate electricity near or at the place it will be used such as hydropower, solar photovoltaic panels, wind, combined heat and power systems and others. The first grid in the early days of electricity generation was a DC-based which



only can supply electricity to neighbourhood living nearby the power plant over short distances. However, as technologies evolved, AC grids began to emerge which allows more power output generation unit to be transported over long distances with good economical benefits. Distributed generation is introduced due to its environmental concerns as they produce little amount of pollution and act as backup supply of electricity to the grid in case of emergency.

The interfacing action between DG units and utility grid is performed by inverter. Different characteristics of distributed generation will form different power quality issues. Power quality problem might arise from the uncontrolled use of power electronic devices, thus reduce the efficiency of the system. Synchronization of grid frequency, voltage imbalance and level of harmonic distortion are some of the serious challenges that need to be overcome in distributed generation system. Due to these reasons, many control methods had been proposed by researchers to conquer the issues mentioned. One of them is PI current controller which has been utilised to mitigate the high harmonics content in the current signals in a DC-AC voltage source inverter interfacing with the grid system [9]. In this case, the DC-AC inverter plays a vital role in providing bidirectional power flow while the step up converter controls the DC link voltage that contributes to power quality improvement of the system.

The logo for UWP (University of Wollongong) is a large, stylized 'U' shape composed of several overlapping triangles in shades of teal and light blue. The letters 'UWP' are printed in a bold, white, sans-serif font across the center of the 'U' shape.

UWP

## 2.2 Inverter Classification

Inverter is responsible for the conversion of DC to AC in grid-connected PV system. Proper phase, frequency and voltage magnitude are highly crucial for synchronization between the AC output signal of PV system with the grid. Power electronics based grid side converter can be divided into two types; line commutated and self-commutated inverters.

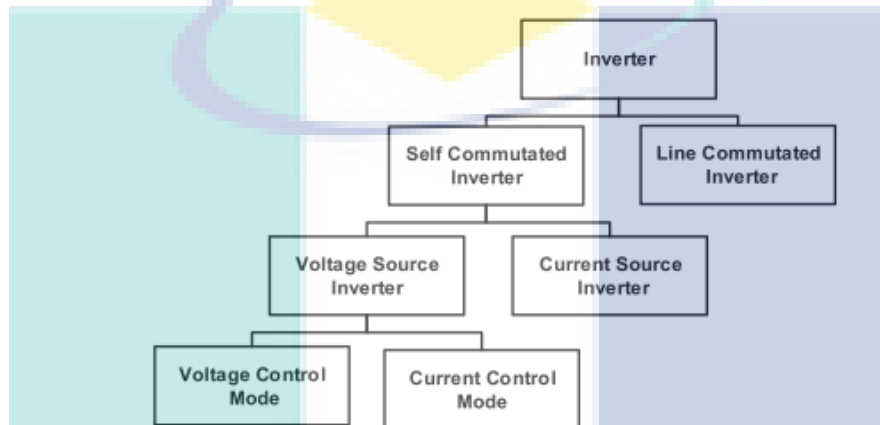


Figure 2.2 Power electronic based converter classification [28]

The difference between these two converters is the switching operation. The switches in line commutated inverter functions based on the direction of current flow whereas self-commutated inverter can fully control the switching process. Both inverters can be further classified into their subtypes as illustrated in Figure 2.2.

### 2.2.1 Voltage Source Inverter

Voltage source inverter is classified as a type of self-commutated inverter where the polarity of input voltage remains unchanged as DC voltage source is located at the input of inverter. At the output side, constant amplitude with AC voltage waveform can be obtained through VSI. Figure 2.3 indicates the structure of self-commutated VSI inverter with the tie-line inductor used to regulate the current flow from inverter to the utility grid.

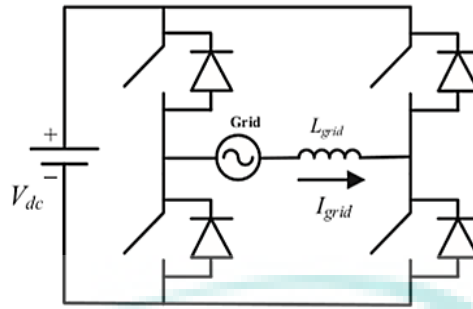


Figure 2.3 Self-commutated VSI inverter [28]

The differences between voltage source inverter (VSI) and current source inverter (CSI) are highlighted in Table 1-1 below. VSI can operate in two modes known as Voltage Control Mode and Current Control Mode. The difference between both modes is that VCM has no control on line current, which is the opposite of CCM. In this project, we prefer to implement VSI operating in current control mode for grid-connected inverter system due to several reasons. One of them is CCM provides more reliable PV power deliverance and safer to operate due to availability control on current. Another reason is that CCM can achieve high power factor and prevent transient current during grid disturbances.

Table 1-1 Comparison between VSI and CSI [28]

Parameters	VSI	CSI
Power source	DC voltage source with lower impedance.	DC voltage source with higher impedance.
Load dependency	Output current magnitude and waveform depends on nature of load.	Output voltage magnitude and waveform depends on nature of load.
Power losses	Low conduction loss with high switching loss leads to low power loss.	High conduction loss with low switching loss leads to high power loss.

### 2.2.1.1 Single Phase Inverter

The transformation of direct current (DC) to alternating current (AC) in the form of electrical energy under acceptable frequency ranging from 50Hz to 60Hz is called inverter. Uninterruptible power supply and AC motor drives are some of the examples of DC-AC inverter in industrial applications. A basic single phase inverter usually consists of DC source as input and IGBT or MOSFET as switch device that are connected to load terminal.

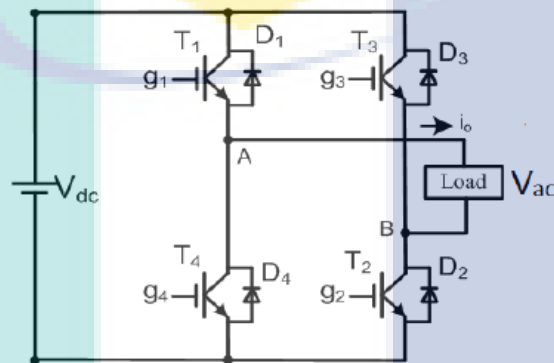


Figure 2.4 Single phase full-bridge inverter IGBT [15]

Three current control techniques known as hysteresis, Proportional-Integral (PI) and ramp-time controller had been tested in shunt active power filter to compare the level of harmonics distortion [13]. However, hysteresis and PI controller are the main focus in our system due to its simplicity and easier to understand. The reason why PI controller is being chosen in the APF system is to keep DC bus voltage constant by regulating the required amplitude of reference current. PI controller tends to have lower harmonics if properly tuned when compared to hysteresis controller. In the APF system, hysteresis controls the motor currents in AC machines and has faster response which makes it robust. In terms of THD level, PI has lesser distortion but gives poor dynamic performance due to non-zero steady state and slow response. In contrary, hysteresis delivers more distortion due to several factors such as variable switching frequency, effect of deadtime and low order harmonics.

### 2.2.1.2 Three Phase Inverter

The structure of three-phase inverter is slightly differ from single phase inverter. By referring to the Figure 2.5 below, three single phase inverter switches are connected to three load terminals with DC source as input. Three-phase inverter is usually applied for high power application (HVDC), variable frequency drive applications and others. A balanced three-phase AC voltages of desired frequency is generated through three-phase square wave inverter. However, the limitation of the three-phase square wave inverter is the output voltage at 5th, 7th and other non-triplen harmonics of fundamental frequency are distorted. This condition might not be tolerable and improper to be applied in filter circuits to filter the unwanted harmonics. Thus, PWM inverter is more preferable as it can produce high quality of output voltage.

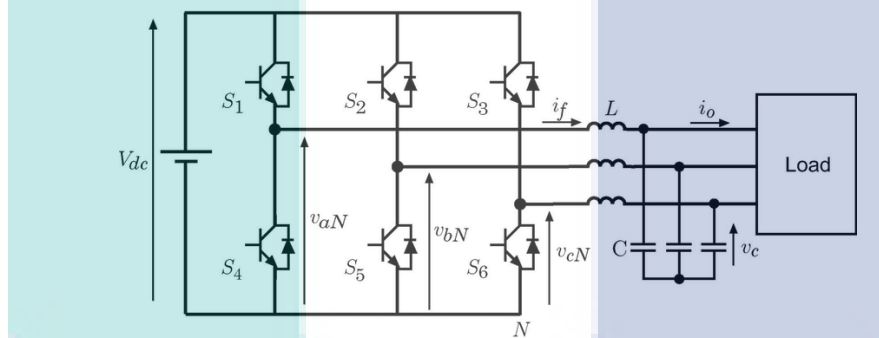


Figure 2.5 Three-phase inverter with LC filter [4]

Two types of current controllers, namely as Proportional-Integral controller and hysteresis controller were tested and compared in terms of THD level in three-phase inverter [4]. From the analysis, PI controller is chosen as the best current controller as it generates better harmonics and rapid current control. Hysteresis controller is second best as it exhibits higher harmonics due to time constant R-L load with some coupling effects. In addition, hysteresis controller produces large frequency range output voltage spectrum and imbalance switching frequency, which is in contrast to PI controller. Despite of it, hysteresis controller still shows good dynamic performance and able to assemble good output current regulation.

## 2.3 Pulse Width Modulation Technique

Producing output voltage with desired frequency and amplitude by generating gate pulses of the inverter's switches is the main purpose of PWM. Unwanted harmonics and switching losses can also be eliminated by using PWM technique [17]. The control of PWM inverters is possible if the fundamental output voltage is in linear and the existence of frequency and harmonics in output voltage. Among the types of PWM technique includes single PWM, multiple PWM and sinusoidal PWM.

### 2.3.1 Single Pulse Width Modulation

In order to regulate the output voltage of inverter, the width of pulse is adjusted by producing one pulse per cycle in single PWM. The amplitude of reference signal which is represented by rectangular wave is compared with the carrier signal of triangular wave to generate gate signal as shown in Figure 2.6 below.

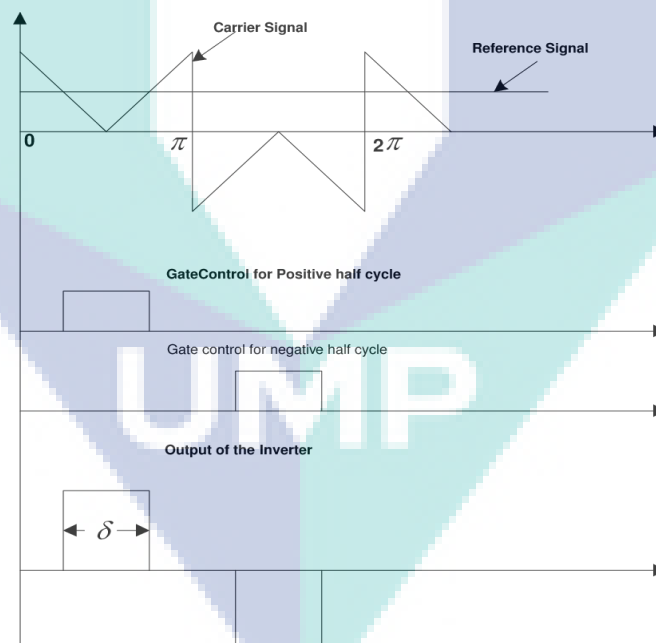


Figure 2.6 Single PWM output [15]

The frequency of carrier signal affects the frequency of output voltage. A ratio known as modulation index is used to adapt the pulse width between reference signal magnitude and carrier signal magnitude during positive and negative cycle.

### 2.3.2 Multiple Pulse Width Modulation

Unlike single PWM, the pulses for one cycle in multiple PWM is increased to reduce the harmonic distortion in waveform, thus leads to higher switching frequency. As shown in Figure 2.7 below, bipolar signals are used in the multiple PWM which are triangular carrier signal and rectangular reference signal. Both signals are compared to produce pulse per half cycle through carrier signal frequency. The gate control on output of inverter is determined by the modulation index.

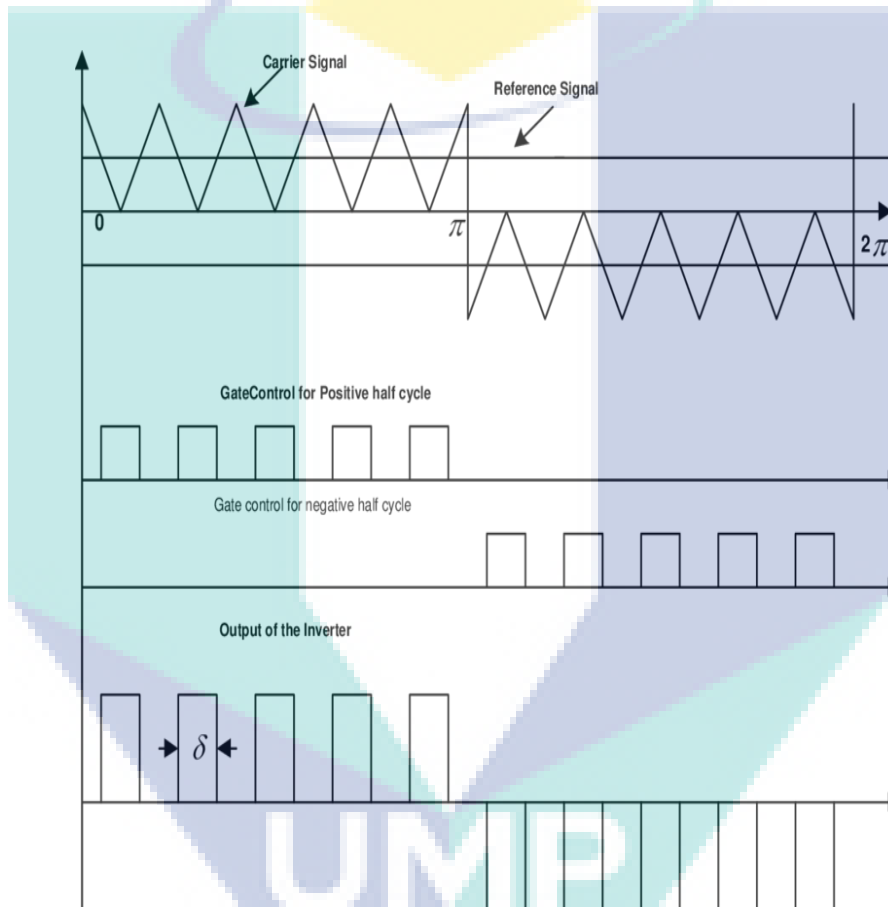


Figure 2.7 Multiple PWM output [15]

### 2.3.3 Sinusoidal Pulse Width Modulation

The PWM technique used in the project is carrier-based PWM which is sinusoidal PWM (SPWM). In order to determine the switching states of inverter, the sinusoidal AC voltage reference,  $V_{ref}$  is compared with the triangular carrier wave,  $V_c$ . When  $V_{ref}$  is higher than  $V_c$ , the upper switch is turned on and the lower switch is turned on when  $V_c$  is larger than  $V_{ref}$ . The output for SPWM is illustrated in Figure 2.8 below.

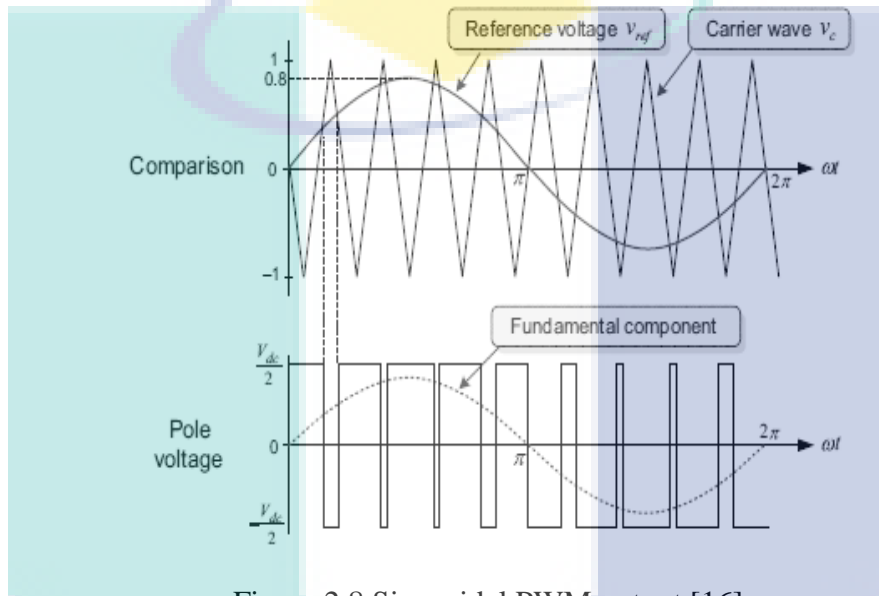


Figure 2.8 Sinusoidal PWM output [16]

SPWM has a constant switching frequency that makes it possible to minimise switching losses. The application of SPWM method had been used in single phase inverter connected to grid by applying the combination of PI with hysteresis controller to analyse the performance of the inverter [3]. The conventional hysteresis controller produce more distortion in grid current as the bandwidth of the hysteresis band increases when compared to PI with hysteresis controller. Although bandwidth of hysteresis band is large, PI with hysteresis controller is able to reduce switching frequency thus leads to more sinusoidal current in the grid and lesser THD level. Simulation of SPWM technique in three-phase inverter had also been presented in MATLAB Simulink to obtain sinusoidal waveform for output voltage [4]. The method is proven to be able to reduce THD in output voltage thus improve the efficiency of inverter.



## 2.4 Grid-Tie Inverter System

Power quality control becomes more serious when the critical load is a nonlinear load. Thus, the waveform quality of grid current is reduced due to the non-sinusoidal characteristics of load. The basic structure of single phase VSI grid tie inverter under nonlinear load condition is presented in Figure 2.9.

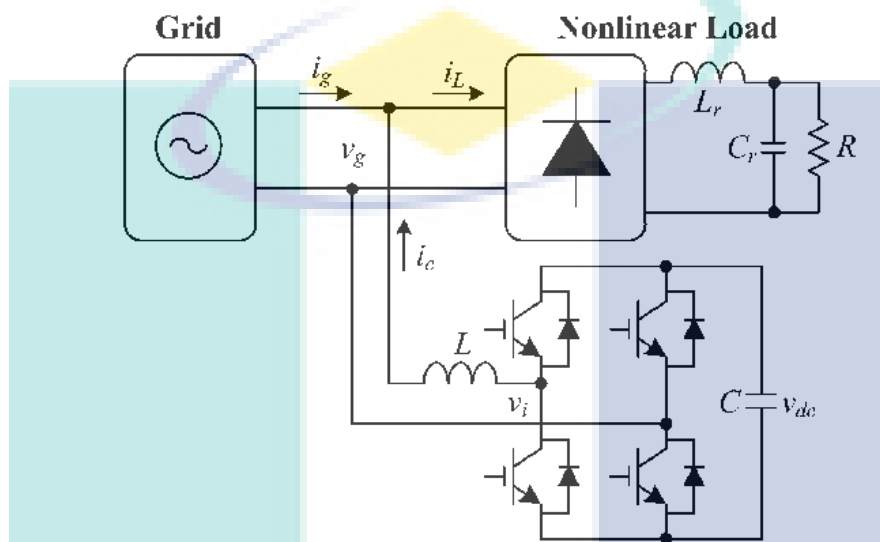


Figure 2.9 Single-phase VSI grid tie inverter under nonlinear load schematic diagram [2]

The consequences of nonlinear load on the grid current is studied in [2] under standalone and grid-connected mode. Diode rectifier (R-C) load act as the nonlinear load as it is the most common modern appliances used nowadays. Nonlinear load current contains large harmonics that causes the grid current to have large harmonics too. However, after PI current control strategy had been applied in standalone and grid-connected mode, the THD of grid current decreases about 3%.

### 2.4.1 Classification of Grid Synchronization Method

As the grid is integrated to inverter system, there are several control issues that need to be solved in order to accomplish stable and robust system. One of them is the grid synchronization issue. In previous research papers, researchers had proposed few synchronization methods for grid-connected inverter in single phase and three phase system as presented in Figure 2.10.

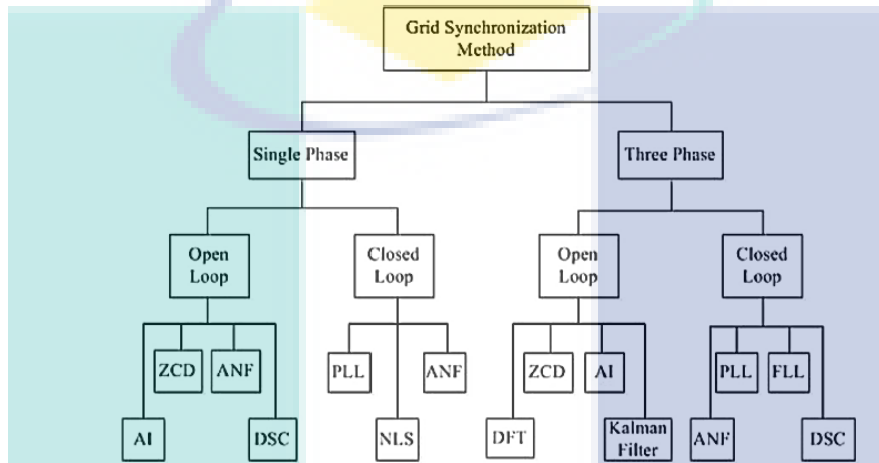


Figure 2.10 Grid synchronization methods for single phase and three phase system [20]

Zero crossing detection (ZCD) method and artificial intelligence (AI) are usually applied in open loop system. ZCD method is prone to frequency variations but additional components are necessary that leads to higher cost [20]. The application of artificial neural network (ANN) through least-square techniques in AI tools contributes to higher rate of convergence and rapid response in power system. Adaptive notch filter (ANF) method offers wide range of benefits such as current harmonics detection and removal of reactive power for power quality control. For unbalanced grid voltage condition, the utilization of delayed signal cancellation (DSC) enables the system to reach zero steady-state error and resistant to frequency variations. Under synchronous reference frame phase locked loop (PLL) method, it allows precise phase angle and frequency estimation but easily affected by sudden change of phase angle which deteriorate the closed loop system performance [22]. Kalman filter technique is not preferable among the other methods due to its complexity of structure and give poor performance under voltage disturbances. Although discrete Fourier transform (DFT) is immune to noise and much

more simpler in structure, the occurrence of phase shift might occur due to mismatch of time window DFT and grid period [20].

## 2.5 Control System

Control system refers to the arrangement of several components to obtain desired output with stable condition, either operates electrically, mechanically, pressure by gas or liquid or all of these combinations. In control system, there are two main configurations which are open loop system and closed loop system.

### 2.5.1 Open Loop System

Open loop system is a non-feedback control system which only takes the input under consideration to generate output. The system also works on fix condition and does not have disturbances or variations. Based on previous papers, inverters that are interfaced to the grid through open loop system does not employs any current controller.

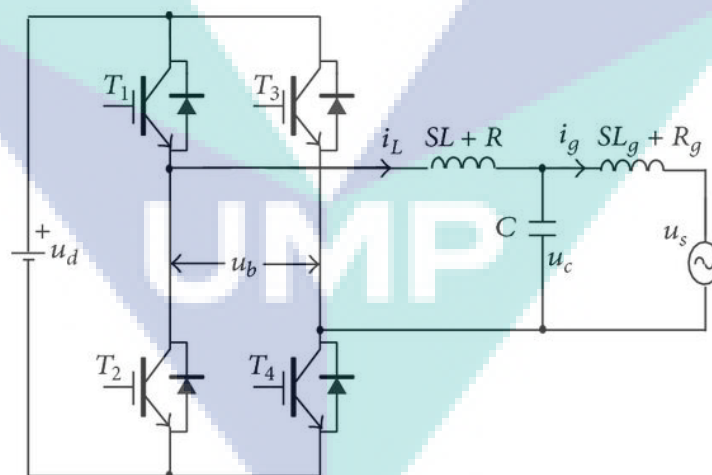


Figure 2.11 LCL-based grid-connected inverter [21]

Other harmonics mitigation method such as low pass filter applies open loop system to operate with inverter connected to grid system. A comparative study between L, LC and LCL filter has been made in order to select the best filter to compensate

harmonics in grid current [21] as shown in Figure 2.11. It is proven that LCL filter has the lowest THD level, followed by LC and L filter. This is due to the fact that LCL filter minimise the inverter current ripples which allows more sinusoidal current to be injected to the grid and sustain power quality standard.

### 2.5.2 Closed Loop System

Unlike open loop system, a closed loop system is a type of feedback control system which tracks the output instead of the input and alters it according to the desired condition. Closed loop system is more difficult to implement due to its complexity of control structure. Moreover, closed loop system requires more components that leads to higher cost compared to open loop system.

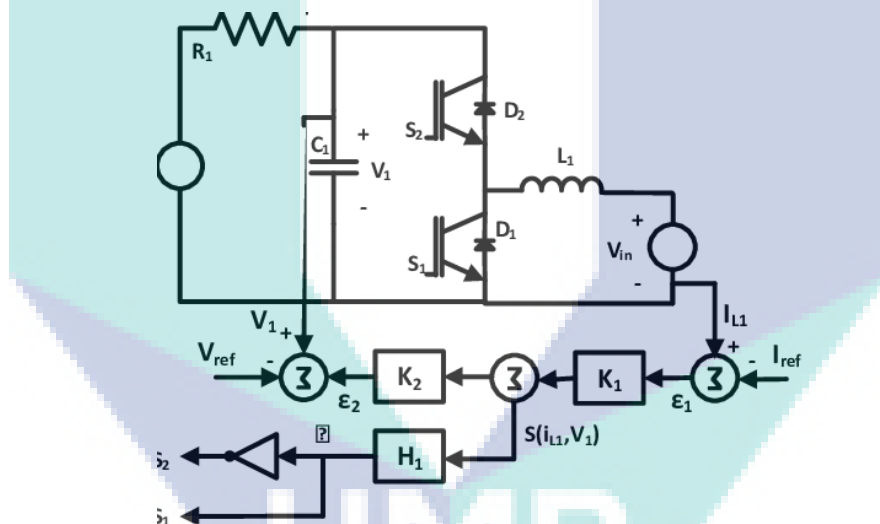


Figure 2.12 PI with hysteresis in single phase boost inverter [11]

However, closed loop system is more favourable when improving the stability of unstable system and adjusting the inputs to reduce errors. The combination of PI and hysteresis controller had been implemented in single phase boost inverter as the testing platform as presented in Figure 2.12 [11]. PI is integrated to the voltage loop control while hysteresis uses current loop control. After comparing the final result with sliding mode controller, the combination of PI and hysteresis controllers had managed to reduce more ripple in output current and voltage that contributes to lower harmonics in current and voltage.

## 2.6 Classification of Current Controllers

Referring to Figure 2.13 below, current controllers can be categorized into two types; linear and non-linear controller. In linear control, the current error and voltage modulation are in separated form. This concept leads to a fixed switching frequency that become one of its advantages. For nonlinear control, the switching frequency is largely affected by the load parameters and change in AC voltage.

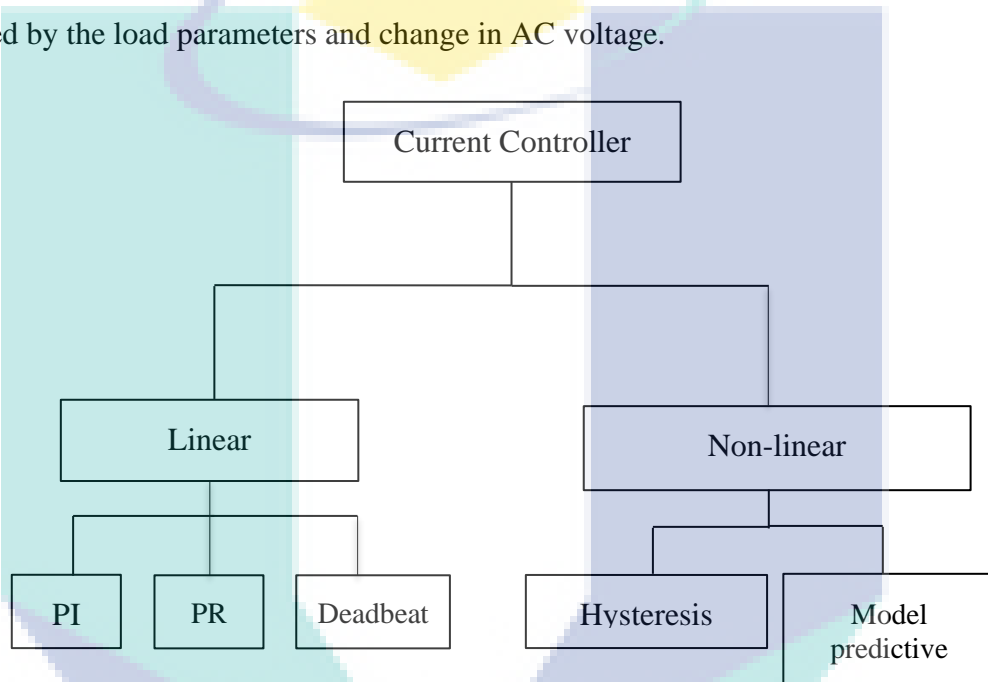


Figure 2.13 Classification of linear and non-linear current controllers for single phase VSI [1]

Different types of controllers serves different purposes, depending on the requirement of system. In grid-connected inverter system, current controllers are essential in adjusting the power exchange between the VSI and utility grid. The current controllers also should be able to enhance better state of waveform, thus increase the power quality of the system.

To differentiate between current controllers mentioned in Figure 2.13, a table of comparison is made for easier understanding as demonstrated in Table 2-2 below.

Table 2-2 Comparison of current control methods

<b>Current</b>			
<b>Control Method</b>	<b>Design structure</b>	<b>Advantages</b>	<b>Disadvantages</b>
Hysteresis [10], [13]	<ul style="list-style-type: none"> <li>- Use natural reference frame.</li> <li>- Does not require PWM block.</li> </ul>	<ul style="list-style-type: none"> <li>- Ease of implementation.</li> <li>- High dynamic response.</li> </ul>	<ul style="list-style-type: none"> <li>- Variations in switching frequency.</li> </ul>
PI [10], [13]	<ul style="list-style-type: none"> <li>- Use synchronous (d-q) frame.</li> <li>- Require PWM block.</li> </ul>	<ul style="list-style-type: none"> <li>- Fixed switching frequency.</li> <li>- Better transient response.</li> </ul>	<ul style="list-style-type: none"> <li>- Non-zero steady state error.</li> </ul>
PR [1]	<ul style="list-style-type: none"> <li>- Use natural reference frame.</li> <li>- PWM block is obligatory.</li> </ul>	<ul style="list-style-type: none"> <li>- Simple design.</li> <li>- Good reference current tracking.</li> </ul>	<ul style="list-style-type: none"> <li>- Invulnerable to variations of system frequency.</li> </ul>
Deadbeat [1]	<ul style="list-style-type: none"> <li>- Use natural reference frame.</li> <li>- PWM block is essential.</li> </ul>	<ul style="list-style-type: none"> <li>- Efficient for mitigation of harmonics.</li> <li>- High dynamic response.</li> </ul>	<ul style="list-style-type: none"> <li>- Responsive to change in system parameters.</li> </ul>
Model predictive [1]	<ul style="list-style-type: none"> <li>- Use natural reference frame.</li> <li>- PWM block is absent.</li> </ul>	<ul style="list-style-type: none"> <li>- High dynamic response.</li> <li>- Easy hardware implementation.</li> </ul>	<ul style="list-style-type: none"> <li>- Require additional mathematical computation.</li> </ul>

### 2.6.1 Hysteresis Controller

Hysteresis controller is the another type of current controller that is commonly applied in control system application due to its directness and fast response. Hysteresis controller depends both on current and past environment. One of the disadvantages of hysteresis controller is that it has high switching frequency which leads to undesirable harmonics. Figure 2.14 and Figure 2.15 below shows the hysteresis controller block diagram and switching pattern of hysteresis control.

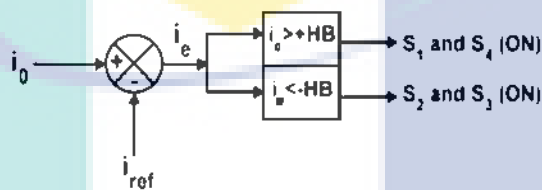


Figure 2.14 Hysteresis controller block diagram [5]

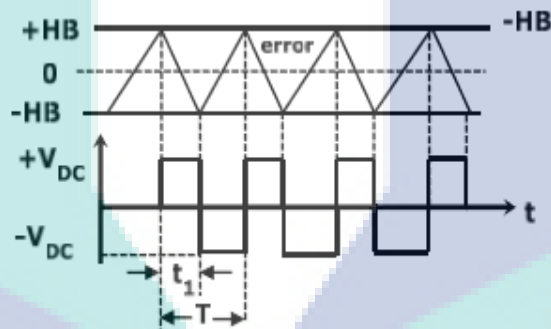


Figure 2.15 Switching pattern of hysteresis control [5]

A modified hysteresis controller is presented to reduce switching losses in grid-connected inverter system [5]. With double-loop control of inverter, the hysteresis controller is proven to have the ability to minimise switching losses without sacrificing output current waveform. Comparison in terms of average switching frequency between proposed hysteresis controller and conventional one with single-band and double band in single-phase full bridge inverter has also been done in [19]. The proposed hysteresis controller had the lowest average switching frequency as single-band hysteresis is said to encounter higher switching frequency and failed to supply zero level output voltage for inverter. Due to high switching frequency of transistors in three-phase inverter, sequential design of hysteresis controller is implemented as in [12] to minimise switching losses. At

frequency of 50Hz and 450Hz, the proposed hysteresis controller exhibit good spectral quality operating under variable switching frequency.

### 2.6.2 Proportional Integral

Proportional Integral (PI) controller is the most ordinary and widely used controller due to its simplicity and better stability in control system. P controller adds integral component in transfer function to eliminate steady state error.

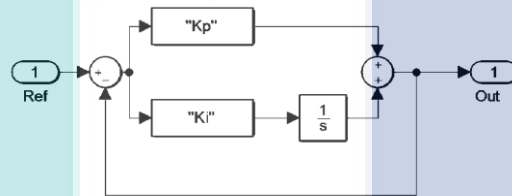


Figure 2.16 Proportional-Integral controller block diagram [18]

The application of PI controller can be seen in single phase inverter that is connected to non-linear load [18]. Inverter and non-linear load generate unwanted harmonics distortion which cause reduction in power quality. Trial and error tuning technique is implemented in the inverter system to obtain optimum gain values of  $K_p$  and  $K_i$ . As the PI controller is applied under non-linear load condition, the total harmonics distortion (THD) shows decrease in value.

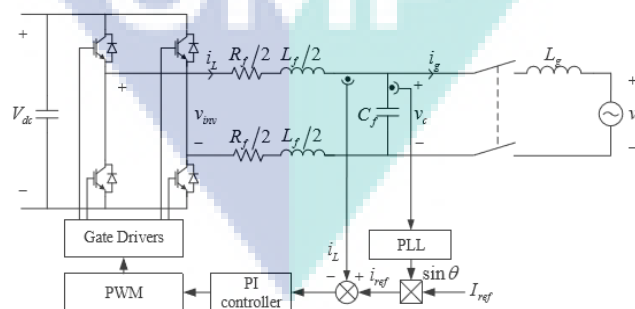
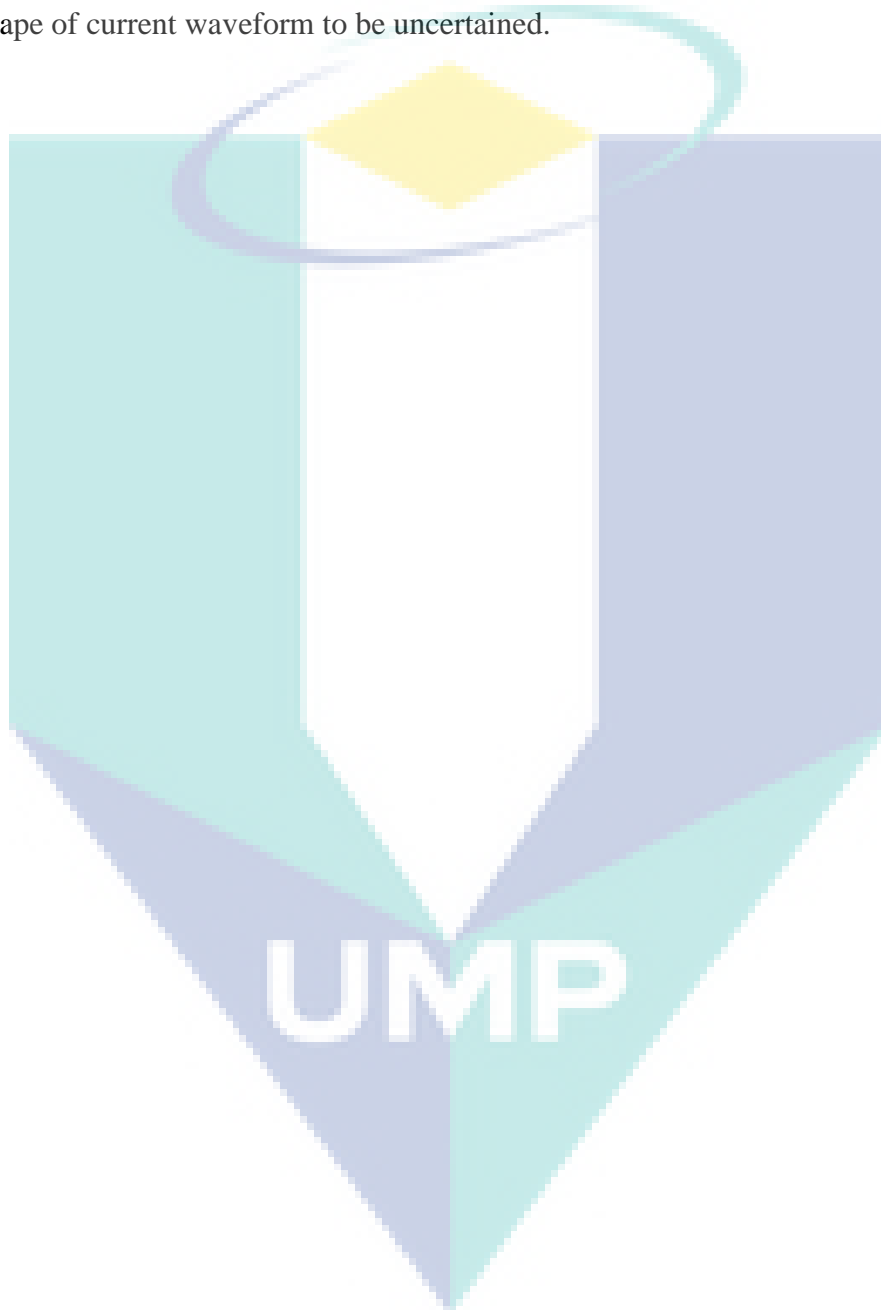


Figure 2.17 Single-phase grid connected inverter with PI controller structure [25]

Good quality current injected into the grid can also be achieved through modified PI controller [25]. This is done by eliminating the steady state error in closed-loop system.



THD analysis shows that the modified PI control is lower than the conventional one which proven to be effective in eliminating steady state error. The performance of proposed PI controller in pulse-width modulation voltage source inverter has also been studied under non-ideal conditions with three-phase induction motor act as load (9). For load outage condition, the proposed PI controller lose its control capabilities and causes the shape of current waveform to be uncertained.



## CHAPTER 3

### METHODOLOGY

#### 3.1 Flowchart of Project

The process for every stage of project can be shown in Figure 3.1. The first stage is the design stage, where the simulation of project is designed based on previous research paper. Then, testing is done in the latter stage to examine the impact of the testing platform under certain condition. Next is the analysis stage where the system performance of controllers are compared in order to choose the best control method used in the project. The last stage is the verification of the system, whether the results obtained are valid by complying with the actual standard as a reference.

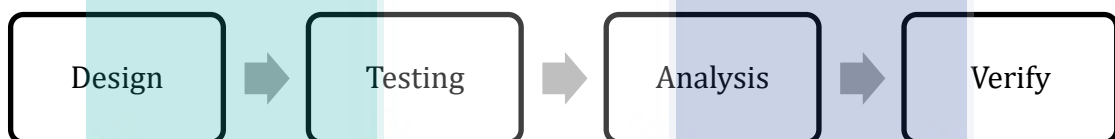


Figure 3.1 Stage-by-stage development of project

The process can be further explained as follows:

(a) Design stage

- Design single phase VSI with LC filter.
- Design grid system by adding AC voltage source operating under 50 Hz.

(b) Testing stage

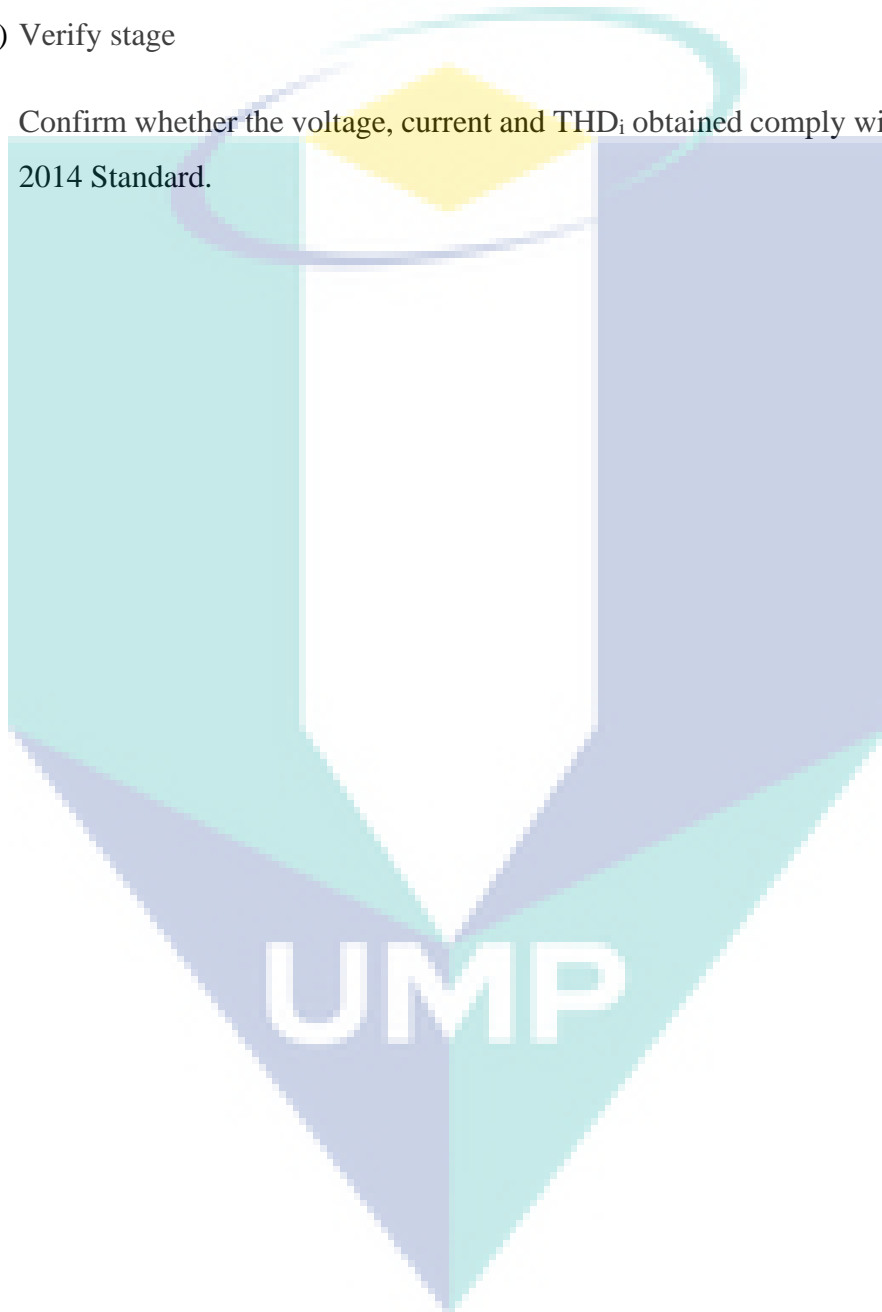
- Examine the effects of voltage and current waveform by adding nonlinear load in the testing platform.

(c) Analysis stage

- Compare and evaluate the system performance of current control methods used to compensate the distortion in grid current waveform by measuring the  $\text{THD}_i$  level.

(d) Verify stage

- Confirm whether the voltage, current and  $\text{THD}_i$  obtained comply with IEEE 519-2014 Standard.



For better understanding of flow of the project, the process is summarised in the form of flowchart as illustrated in Figure 3.2.

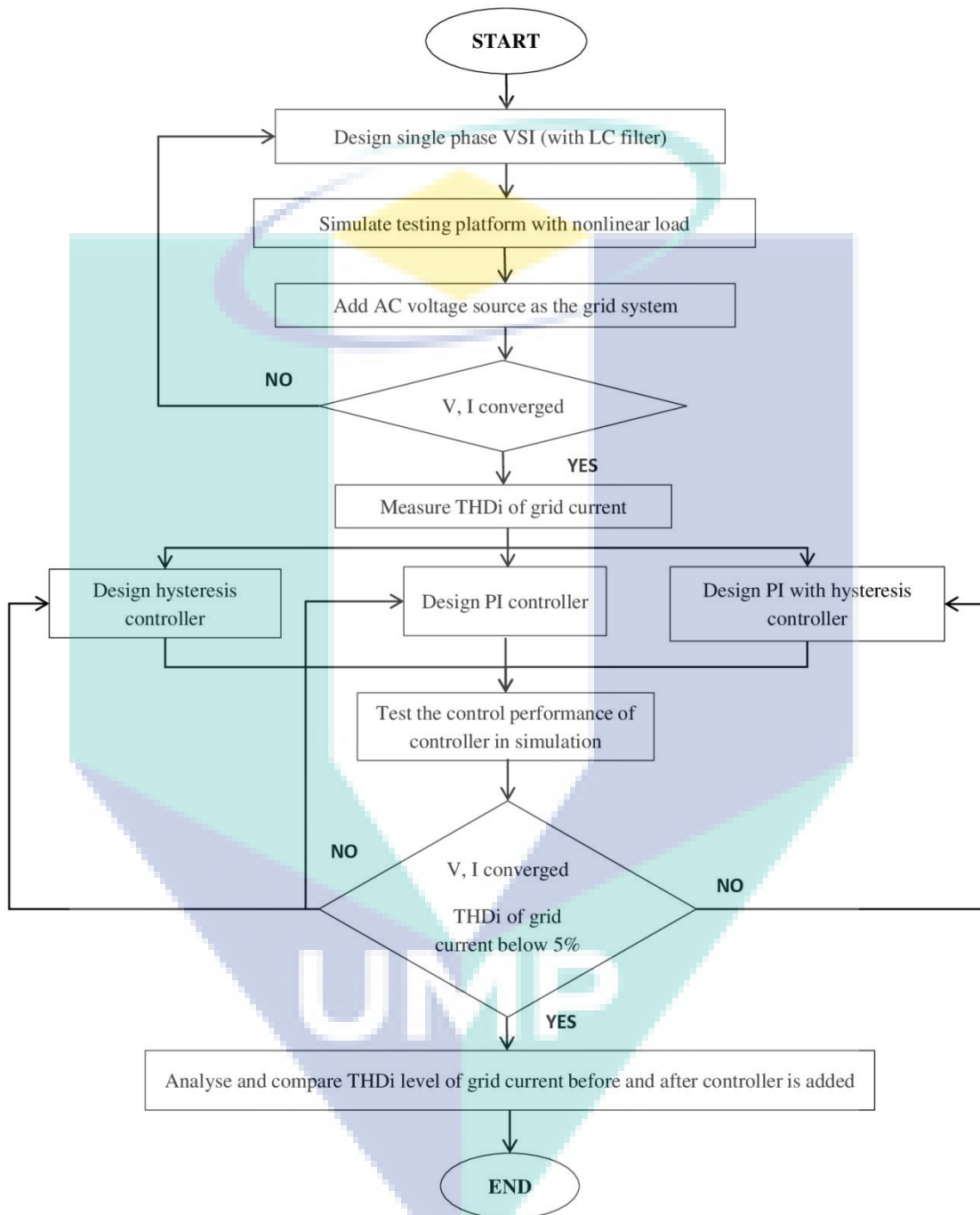


Figure 3.2 Overall flowchart of project

### 3.2 Block Diagram of Overall Project

Referring to block diagram in Figure 3.3, this project consists of several parts. PCC is described as the common point of coupling where multiple loads are connected to the same terminal.

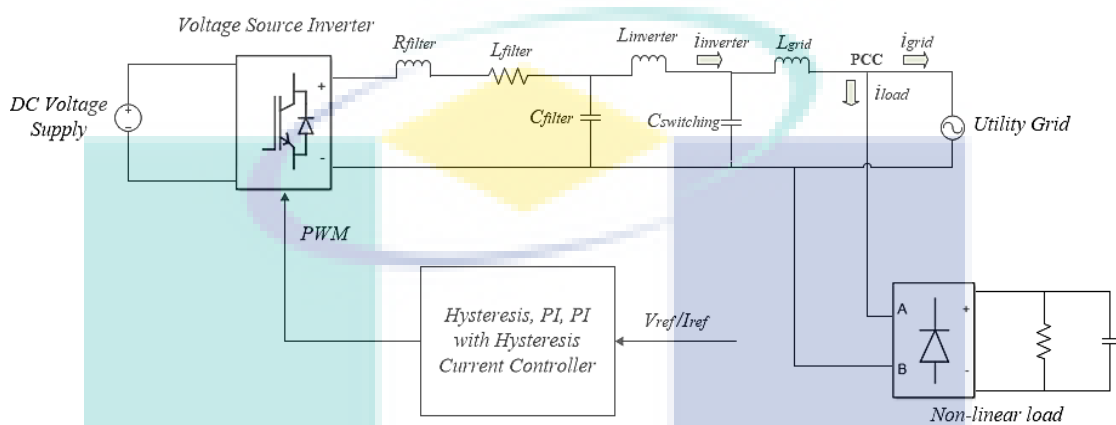


Figure 3.3 Block diagram of project

The components and function of each parts are as below:

- i. DC Voltage Supply
  - Supply voltage to be fed to the voltage source inverter.
- ii. Voltage Source Inverter
  - Convert DC to AC voltage to be delivered into the utility grid.
- iii. Utility Grid
  - Transmit electricity over distances to be distributed to consumer via step-down transformer.
- iv. RLC filter (  $R_{filter}$ ,  $L_{filter}$ ,  $C_{filter}$  )
  - To filter out switching harmonics of PWM.

- v. Switching capacitor,  $C_{switching}$ 
  - Remove switching components on point of common coupling (PCC) from entering the grid.
- vi. Inverter inductance,  $L_{inverter}$ 
  - Allow ripples in source current.
- vii. Grid inductance,  $L_{grid}$ 
  - Act as the grid impedance.
- viii. Non-linear load
  - Draws distorted harmonics current to the grid.
- ix. Hysteresis current controller, PI controller and PI with hysteresis current controller
  - Compensate the harmonics content in grid current.
- x. Pulse Width Modulation (PWM)
  - Compare reference voltage/current and measured voltage/current to generate bipolar PWM to be fed into the inverter.



UMP

### 3.2.1 Simulation Parameters

Table 3-1 summaries the parameters used in the system. The DC voltage is set at 250V as it is the most optimum trade-off value. Higher voltage injects cleaner grid current but generate higher losses and expensive components are the major drawback. For lower voltage, the efficiency of system is higher with cheaper components even though it has larger distortion in grid current The grid voltage is fixed at  $110V_{rms}$  operating under 50Hz.

Table 3-1 Simulation parameters of circuit

Parameters	Value
$V_{DC}$	250 V
$V_{Grid}$	110 $V_{rms}$
Line frequency, f	50Hz
Switching frequency, $f_{sw}$	11.1 kHz
RLC filter	$R_f = 0.2 \Omega$ $L_f = 2.5 \text{ mH}$ $C_f = 11 \text{ mF}$
Nonlinear load	$R_{load} = 88 \Omega$ $C_{load} = 470 \mu\text{F}$
Inverter inductance, $L_{inv}$	5 mH
Switching capacitor, $C_s$	15 $\mu\text{F}$
Grid impedance, $L_{grid}$	15 mH

### 3.3 System Design

#### 3.3.1 Single Phase Inverter System Design

Generally, the single phase inverter consists of four IGBTs as the switching devices with DC voltage supply to store power retrieved by converter to be supplied to inverter. IGBT is more preferable due to its high voltage capability and rapid switching speed. In this experiment,  $250V_{DC}$  is supplied to the inverter with switching frequency of 11.1kHz. PWM pulses triggered the IGBTs gates which can be drawn from PWM generator. Figure 3.4 below shows the simulation block of single-phase inverter used in this project.

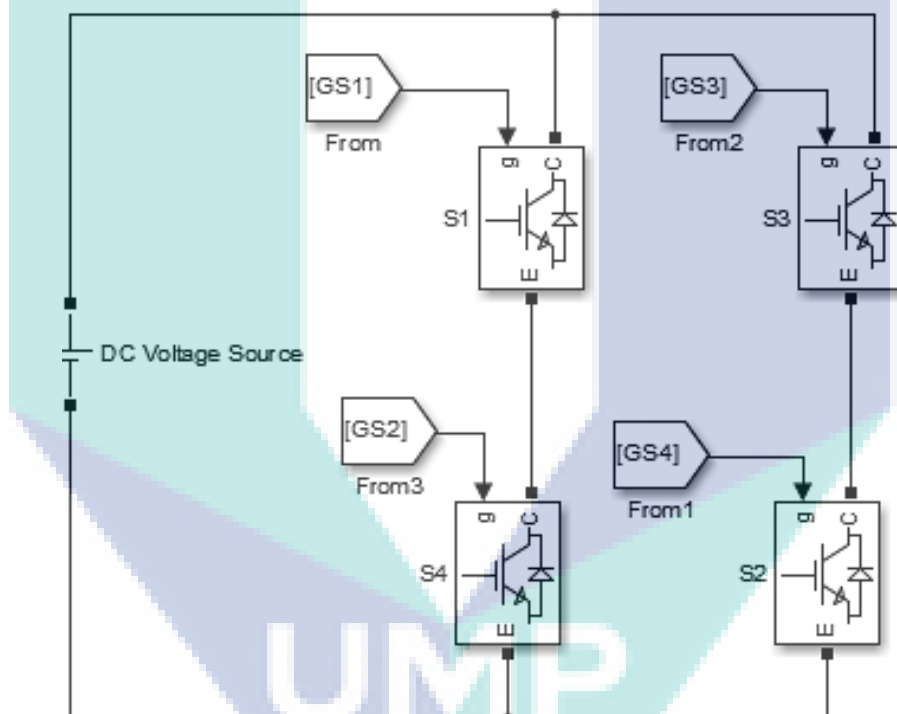


Figure 3.4 Single phase PWM-VSI Simulink block



### 3.3.2 PWM Generator

Based on the Figure 3.5 below, there are two signals being compared in sinusoidal pulse-width modulation (SPWM). Sine wave act as the reference signal will compare with carrier signal represented as sawtooth generator to produce bipolar modulation waveform. In this simulation project, the switching frequency is set at 11.1kHz as it has low switching losses and good stability conduction in typical IGBT switched application. Better current waveform and less audible noise can be generated from higher switching frequency.

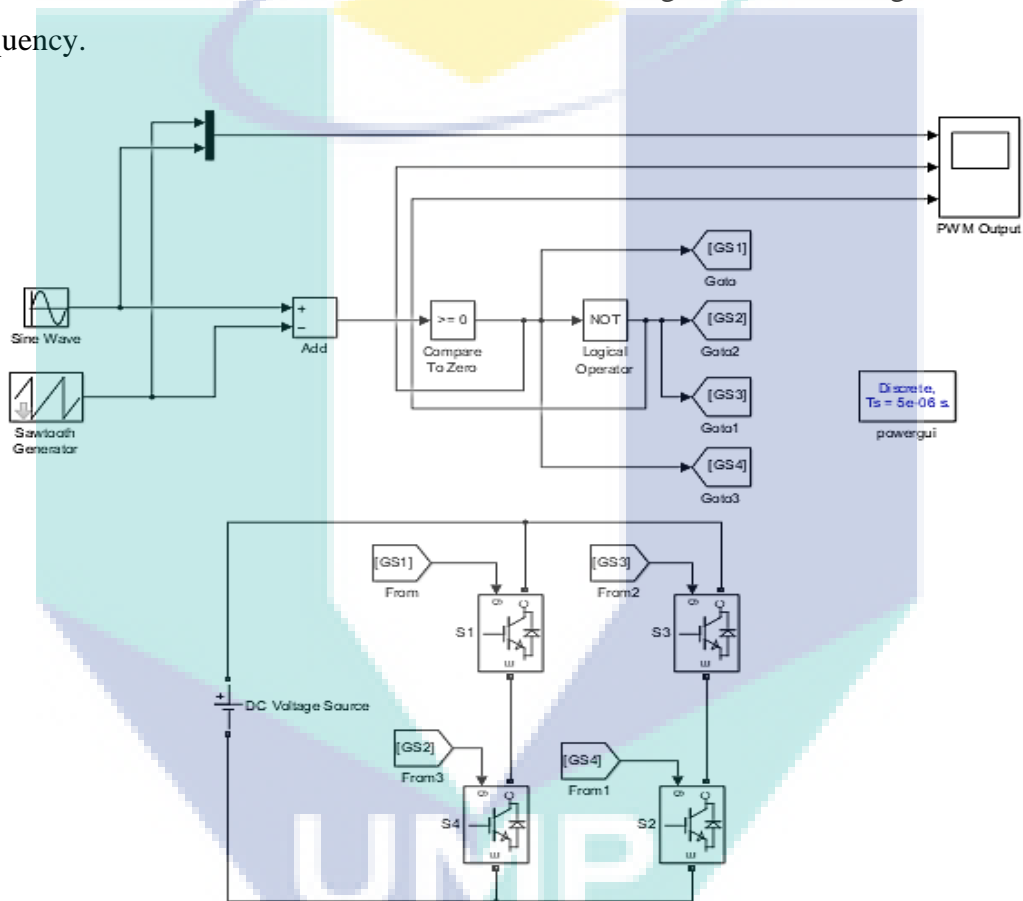


Figure 3.5 PWM generator for single phase inverter simulation block

### 3.3.3 LC Filter Selection

At the output terminal of full bridge VSI, LC filter is very essential in reducing signal's noise or known as harmonics which are produced by pulsating modulation waveform. In order to eliminate most of the low order harmonics, appropriate value for cut-off frequency must be chosen. The output impedance should be kept zero with no

voltage distortion under different load condition. In this project, the overall parameter of filters are  $0.2\Omega$  for resistance,  $2.5\text{mH}$  for inductance and  $0.5\text{mF}$  for capacitor value. Figure 3.6 below shows the simulation blocks of single phase inverter with LC filter in Simulink.

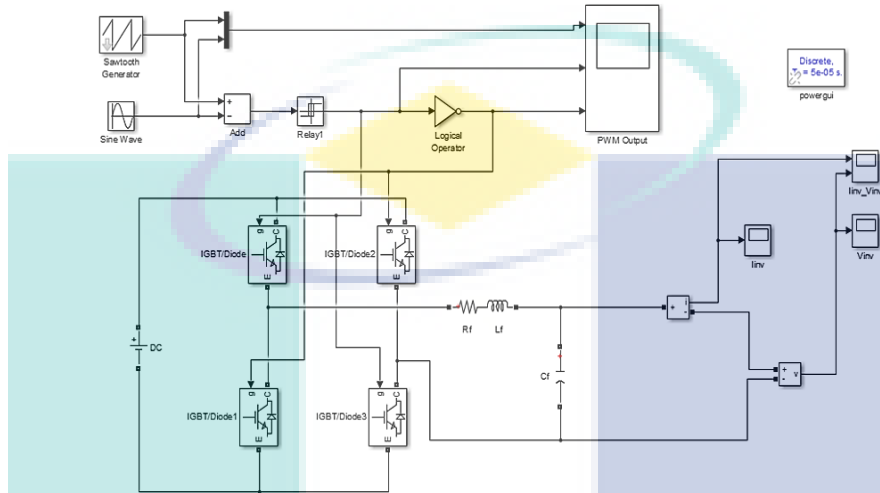


Figure 3.6 Single phase inverter with LC filter simulation block

High capacitance value with low inductance value are the most ideal LC filter to operate at the selected cut-off frequency of the low-pass filter. The first step to design ideal LC filter is determining the impedance by using the below equation:

$$Z_d = \frac{V_{max}}{I_{max}} \quad (3.1)$$

Next step is to calculate the inductance,  $L$  and capacitance,  $C$  values by applying formulas below:

$$L = \frac{Z_d}{2\pi f} \quad (3.2)$$

$$C = \frac{1}{2\pi f Z_d} \quad (3.3)$$

After obtaining inductance and capacitance for the LC filter, the cut-off frequency is finally determined by the equation below. Note that the cut-off frequency is within 5% to 25% of switching frequency.

$$f_c = \frac{1}{\sqrt{LC}} \quad (3.4)$$

Applying the cut-off frequency formula from equation (3.4) above, the cut-off frequency in this system is 1.1kHz.

### 3.4 Non-Linear Load

A diode rectifier load act as the local loads to resemble nonlinear loads such as computers and DC power equipments. The reason why diode rectifier is selected as load is due to its very demanding load in grid-connected inverter system.

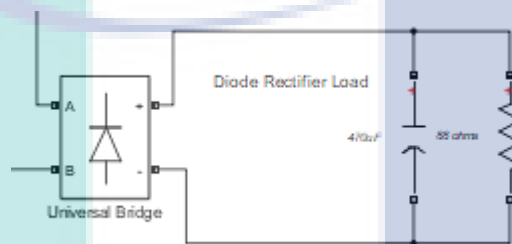


Figure 3.7 Diode rectifier (R-C load) as nonlinear load

Figure 3.7 above is the interconnection of diode rectifier load consists of a resistor and capacitor. As the grid-connected inverter system is connected to nonlinear loads, it causes non-sinusoidal current waveform and harmonics distortion problem. In this project, values of RC load used are  $88\Omega$  and  $470\mu\text{F}$ .

### 3.5 Grid Modelling

Grid impedance is highly dependent on the connected loads and the power grid structure. However, grid modelling based on the impedance measurement is beyond the scope of this work. In this simulation, 10 mH is selected as the grid impedance with 110  $V_{RMS}$  grid voltage supply operating at 50Hz.

For synchronization between the inverter and the grid, this project does not require PLL method. This is because the reference voltage is directly taken from the grid voltage whereas the reference current is taken from the output current of inverter. It means that if the grid voltage is set at  $110V_{RMS}$  operating in 50Hz, the reference voltage is also set at the same voltage and frequency value as shown in Figure 3.8 below.

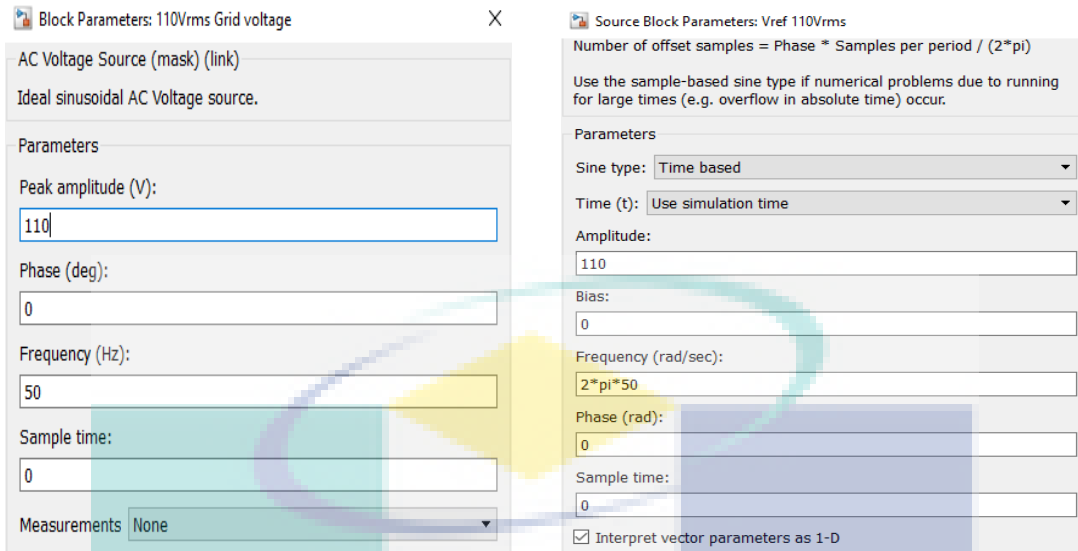


Figure 3.8 Input voltage of grid (left) and reference voltage from grid (right) configuration tab

Through this method, it is more robust and constructive compared to conventional reference signal generation as this method can minimize cost and lessen the number of components such as PLL. Figure 3.9 below illustrates the Simulink block of single phase PWM-VSI connected to grid designed in the project.

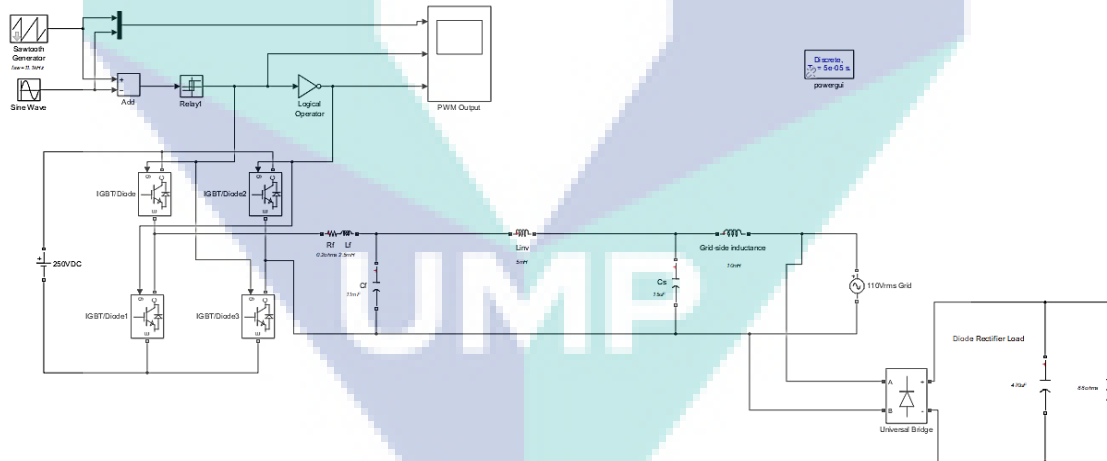


Figure 3.9 Single phase PWM-VSI connected to grid simulation block

### 3.6 Controller Design

Various current control strategies for single phase grid-connected inverter had been proposed by researchers to compensate harmonics distortion in voltage and current waveform such as proportional resonant (PR), deadbeat current control, model predictive current control and many more. In this project, the main focus of current controller used are proportional-integral (PI) controller and hysteresis controller.

#### 3.6.1 Hysteresis Current Controller Modelling

Since hysteresis current control is simple and easy to be implemented, it is widely used in grid-connected inverters. The operation of this control scheme works by comparing the measured output current of the inverter with the reference current. As the controller generates switching pulses for the IGBTs, a fixed hysteresis bandwidth which consists of upper limit and lower limit controls the current error within its range. Switches S1 and S4 are at ON state when the current error reaches the upper limit while S2 and S4 are turned ON if the current error meets the lower limit. In order to achieve desired reference current tracking, the hysteresis bandwidth,  $h$  can be determined by:

$$h = \frac{(V_{dc}^2 - V_{grid}^2)}{4V_{dc}L_{fs}} \quad (3.5)$$

The current error is controlled by calculating the switching frequency of the inverter connected to grid. The switching cycle is expressed by  $0 \rightarrow t_1$  period, where

$$t_1 = T_{ON} = \frac{2L_f HB}{V_{DC} - V_{grid}} \quad (3.6)$$

For  $t_1 \rightarrow T$  period, the equation can be computed as

$$T - t_1 = T_{OFF} = \frac{2L_f HB}{V_{DC} + V_{grid}} \quad (3.7)$$

Based on the equation (3.5), the hysteresis band in this simulation project is set at 2. The simulation modelling of hysteresis controller is shown in Figure 3.10 below. The generation of  $I_{ref}$  is taken from the output current from inverter whereas the measured current is referred to output current from grid,  $I_{grid}$ . The error between both reference and

measured current are controlled in a region containing upper and lower limit called hysteresis band.

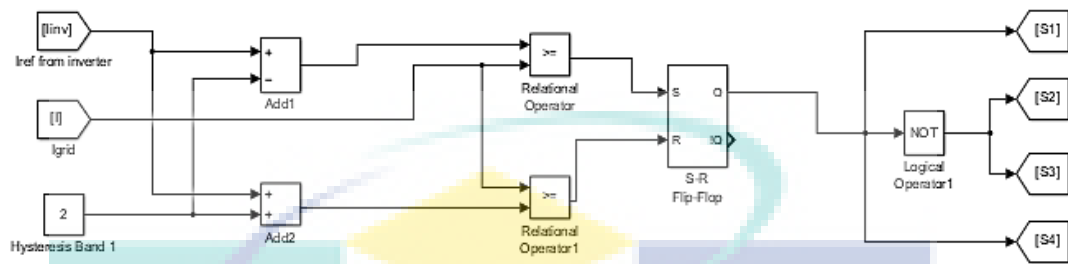


Figure 3.10 Hysteresis controller simulation block

UMP

### 3.6.2 PI Controller Modelling

There are several methods to design PI controller such as Ziegler-Nichols method, pole-placement method, frequency response and others. However, in this system, the design of PI controller is taken from [6]. The transfer function of PI controller can be expressed as :

$$PI(s) = K_p + \frac{K_i s}{s} \quad (3.8)$$

where  $K_p$  refers to Proportional (P) term and  $\frac{K_i s}{s}$  is the Integral (I) term.

The tuning method being applied is trial and error. Since there are two loops of controller,  $K_p$  value in outer voltage control is first increased until it reaches the desired output value, followed by  $K_i$  value until the system achieves steady state. After the  $K_p$  and  $K_i$  values in outer voltage control has been fixed, the  $K_p$  and  $K_i$  values in inner current control are adjusted until the system is stable.

From the trial and error tuning, the  $K_p$  value for both control loop in this system are 1 and 0.1 whereas the  $K_i$  value for both control loops are 0.6 and 0.002. The design structure of PI controller used in this system is shown in Figure 3.11 below. The voltage and current sensor gain are both set at 0.03 and 0.01 respectively.

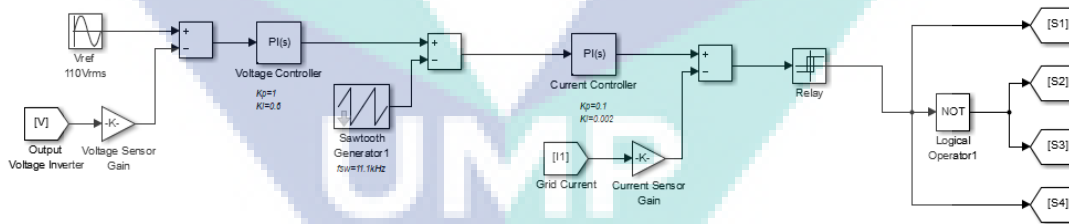


Figure 3.11 PI controller simulation block

### 3.6.3 PI with Hysteresis Current Controller Modelling

Figure 3.12 presents the generation of reference current,  $I_{ref}$  in PI with hysteresis current controller. First, the reference voltage,  $V_{ref}$  which is referred to grid voltage is compared with output voltage of inverter,  $V_{inv}$ . The error generated from both signals are reduced by PI controller.  $I_{ref}$  coming out from the PI controller will be compared with the output grid current,  $I_{grid}$  to be regulated by hysteresis band to produce switching pulses for gate signals..

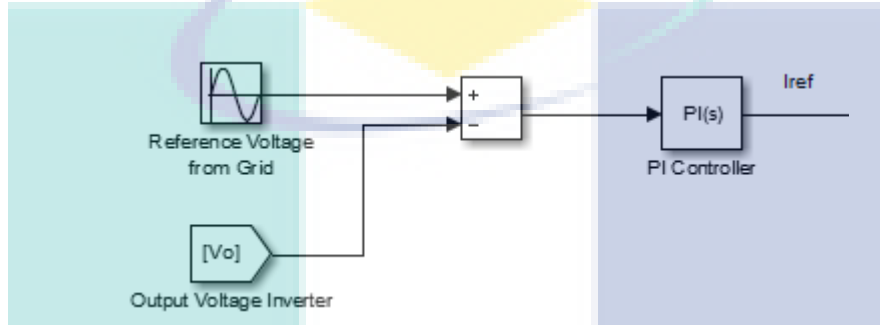


Figure 3.12  $I_{ref}$  generation for PI with hysteresis current controller

The expression for PI controller is equals to

$$PI(s) = K_p + \frac{Ks}{s} \quad (3.9)$$

where  $K_p$  tends to reduce the error between reference current and measured current while  $\frac{Ks}{s}$  controls the oscillation of the system. The reference current that came out from the PI controller will enter the hysteresis band in order to regulate its error within certain range. The output current from inverter can be given as:

$$I_o = i_{ref} + e \quad (3.10)$$

Thus, deviation of error can be written as:

$$\frac{de}{dt} = \frac{V_{dc} - V_{grid}}{L_f} \quad (3.11)$$

As IGBT switch 1 and 4 is ON, the error of current changes from negative HB to positive HB. The ON time interval can be calculated as:

$$T_{ON} = \frac{2L_f HB}{V_{dc} - V_{grid}} \quad (3.12)$$



When IGBT switch 2 and 3 is ON, similar method can be applied where the equation is given as:

$$T_{ON} = \frac{2LfHB}{V_{dc} + V_{grid}} \quad (3.13)$$

By combining equation (3.11) and (3.12), the switching frequency of the system is:

$$f_s = \frac{(V_{dc}^2 - V_{grid}^2)}{4V_{dc}LfHB} \quad (3.14)$$

The value of  $K_p$  and  $K_i$  used in the project is 0.4 and 5.2 respectively through trial and error tuning method while hysteresis band is set at 2. The overall simulink block design of PI with hysteresis current controller is demonstrated in Figure 3.13 below.

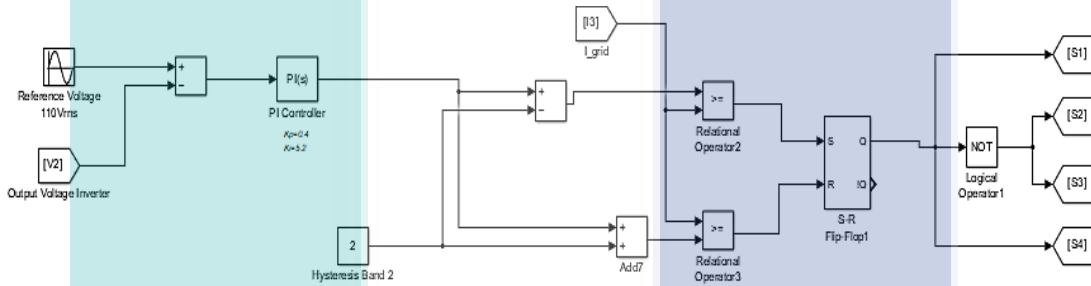


Figure 3.13 PI with hysteresis current controller simulation block

### 3.7 Performance Measures

In this project, the evaluations of the current control techniques are analysed through FFT analysis. Through the analysis, it gives insight about the dynamic performance of the current control techniques.

#### 3.7.1 Total Current Harmonics Distortion (THD<sub>i</sub>)

Harmonics content in a current waveform is measured through  $THD_i$ . It can be expressed as the summation of all harmonics component of the current waveform against the fundamental frequency of current as shown in equation (3.15). This means that the output of a system receives the same fundamental frequency as the input when a sinusoidal input is applied with nonlinear system. Higher percentage of  $THD_i$  indicates that more distortions are present in the waveform.

$$THD_i = \frac{1}{I_{resultant,1}} \sqrt{\sum_{n=2}^{\infty} I_{resultant,n}^2} \cdot 100\% \quad (3.15)$$

Every project should comply with a benchmark set by certain standards. In this project, the standard for current harmonics distortion used is IEEE 519-2014 which stated that  $THD_i$  must below than 5%.

UMP

## CHAPTER 4

### RESULTS & DISCUSSIONS

#### 4.1 Single Phase Full Bridge Inverter with SPWM

In practical, single phase full bridge inverter consists of four semiconductor switches S1, S2, S3 and S4. In this system, the type of switches used is Insulated Gate Bipolar Transistor (IGBT) due to its rapid switching speed, high voltage capability and suitable for high voltage application such as pulse-width modulation (PWM) and DC-AC converter with solar source. Table 4-1 below shows the switching states for single phase VSI.

Table 4-1 Switching states for single phase VSI

S1	S2	S3	S4	S <sub>A</sub>	S <sub>B</sub>	V <sub>o</sub>
ON	OFF	OFF	ON	1	0	V <sub>DC</sub>
OFF	ON	ON	OFF	0	1	-V <sub>DC</sub>

The single phase VSI with SPWM model has been simulated in MATLAB Simulink. The switching frequency sawtooth generator is set to 11.1kHz in the sawtooth generator. To generate SPWM signal, sine wave which act as reference signal compares with high frequency triangular wave. A wave approximately equal to a sine wave and bipolar PWM waveform are produced from the output of full wave bridge inverter with SPWM signal as shown in Figure 4.1.

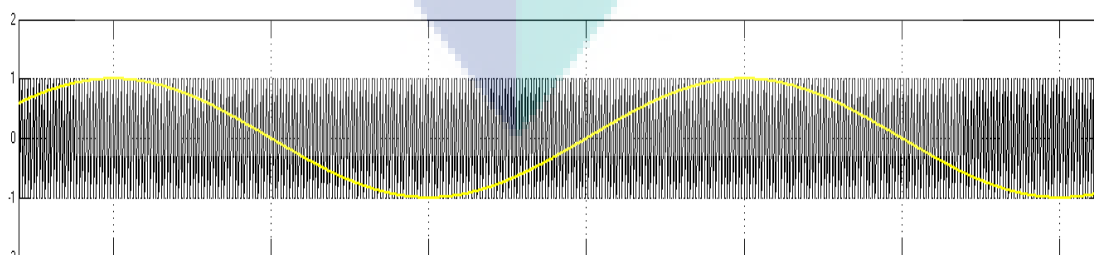


Figure 4.1 Reference signal as sine wave and carrier signal as sawtooth generator

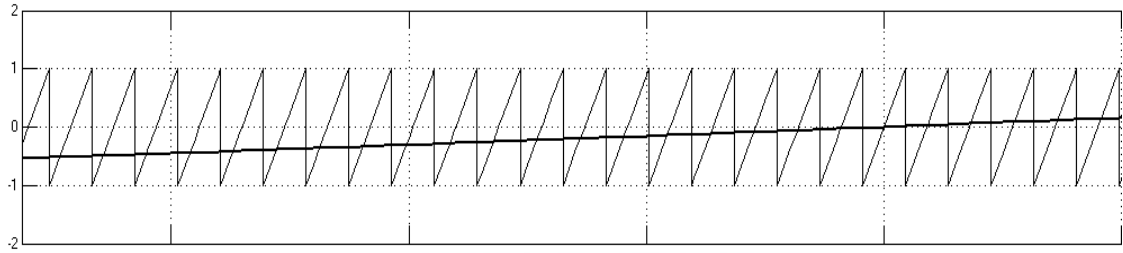


Figure 4.2 Zoom-in view of reference signal with carrier signal

Figure 4.3 illustrates the switching pattern of IGBTs. When S1 and S4 is ON, the output will be 1 while S2 and S3 is in OFF state equals to 0. When S2 and S3 turns ON, output will be -1 and the output of S1 and S4 will be 0 indicating OFF state.

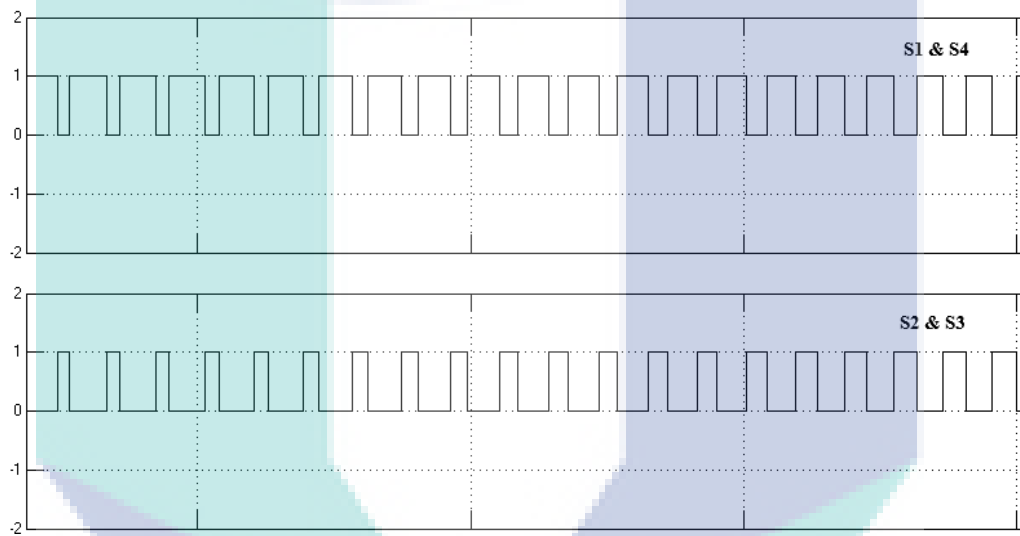


Figure 4.3 Switching states of IGBTs

## 4.2 Single Phase VSI under Nonlinear Load (with LC Filter)

When the VSI with LC filter is connected to nonlinear load, it draws an output voltage inverter of  $185V_{AC}$  from input voltage inverter of  $250V_{DC}$ . As seen in Figure 4.4, the waveform of  $V_{inv}$  is in sinusoidal shape.

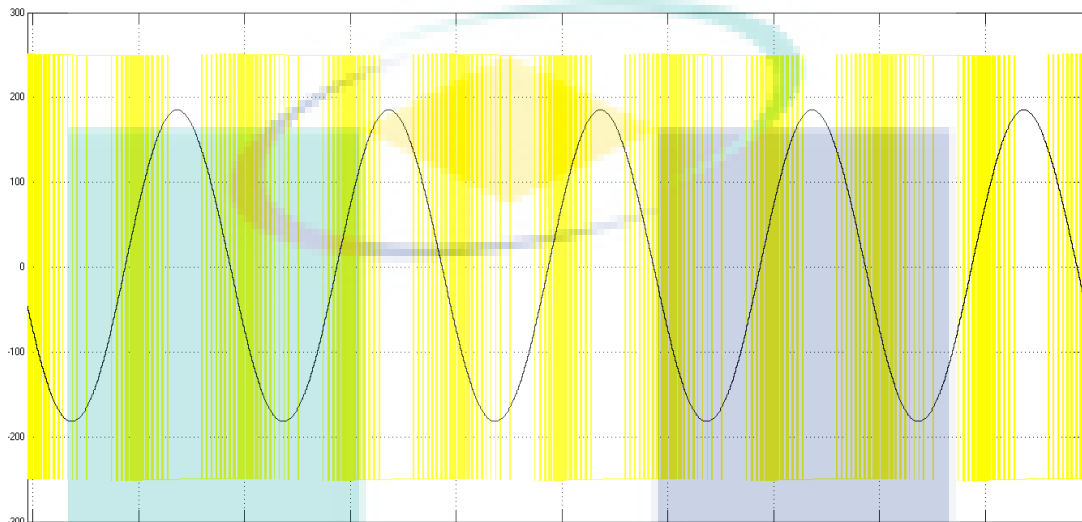


Figure 4.4 Input and output voltage of inverter,  $V_{inv}$

However, it appears that the shape of  $I_{inv}$  waveform as illustrated in Figure 4.5 is slightly distorted due to the characteristics of nonlinear load. It draws an output current inverter of  $21A_{rms}$ .

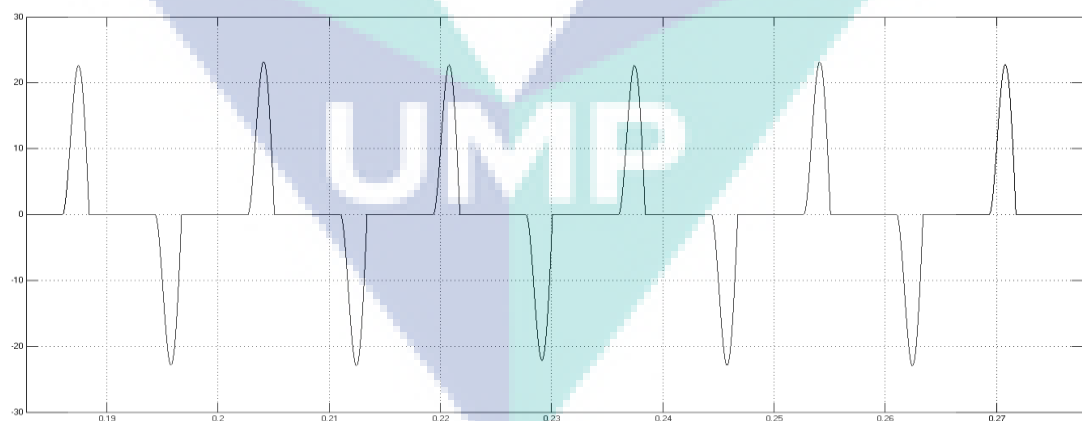


Figure 4.5 Output current of inverter,  $I_{inv}$

The output load current,  $I_{load}$  which draws  $21A_{rms}$  in Figure 4.6 also shows that the non-sinusoidal and distortion waveform affects the nature of the current produced in inverter.

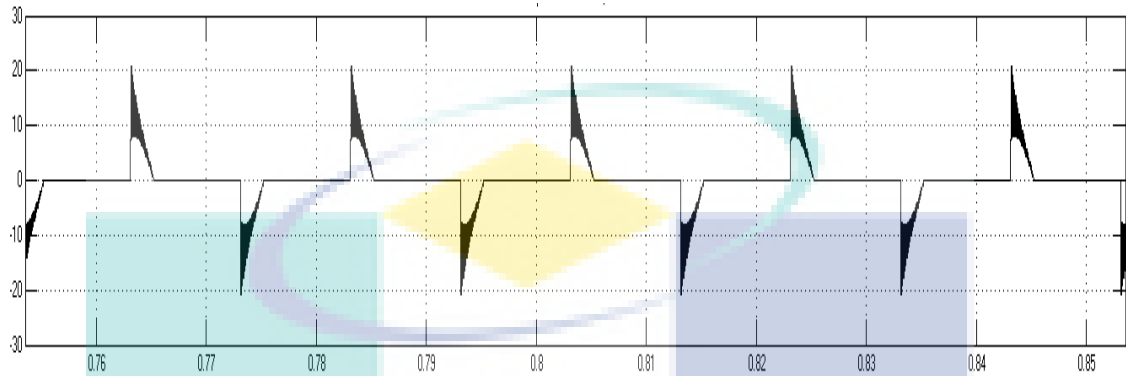


Figure 4.6 Output load current,  $I_{load}$

As expected, nonlinear load tends to have high harmonics content due to its nonlinear characteristics. From the FFT analysis shown in Figure 4.7, when the harmonics order increases, the magnitude of frequency decreases. The  $THD_i$  of  $I_{load}$  in the simulation is approximately 155.55% under fundamental frequency of 50Hz.

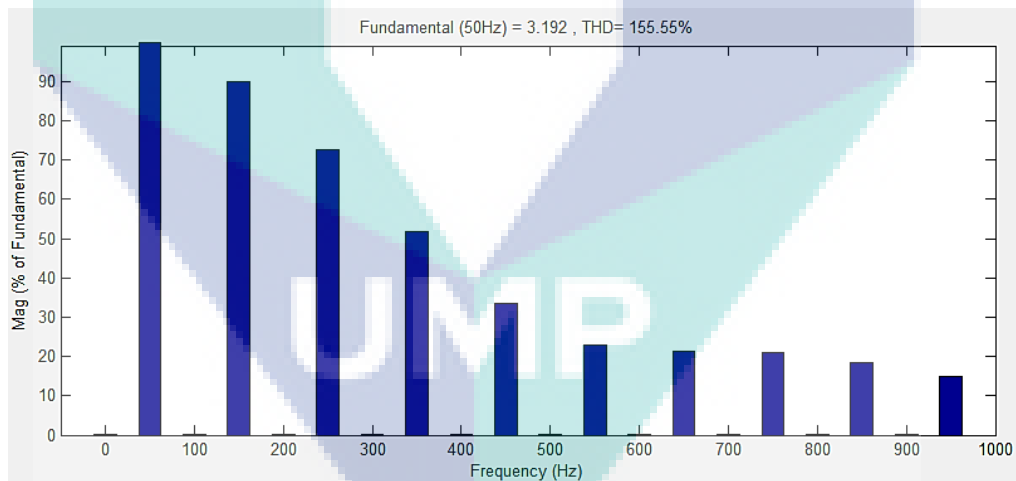


Figure 4.7 Harmonics spectrum of  $I_{load}$

### 4.3 Single Phase VSI Grid-Connected Under Nonlinear Load (Without Current Controller)

As the single phase VSI is integrated with the grid system, the output signals for voltage of inverter presented in Figure 4.8 is in sinusoidal shape with the value of  $132.5V_{AC}$  from  $250V_{DC}$  input inverter voltage. It proves that the waveform shape of output voltage of inverter is not affected by the nonlinear load.

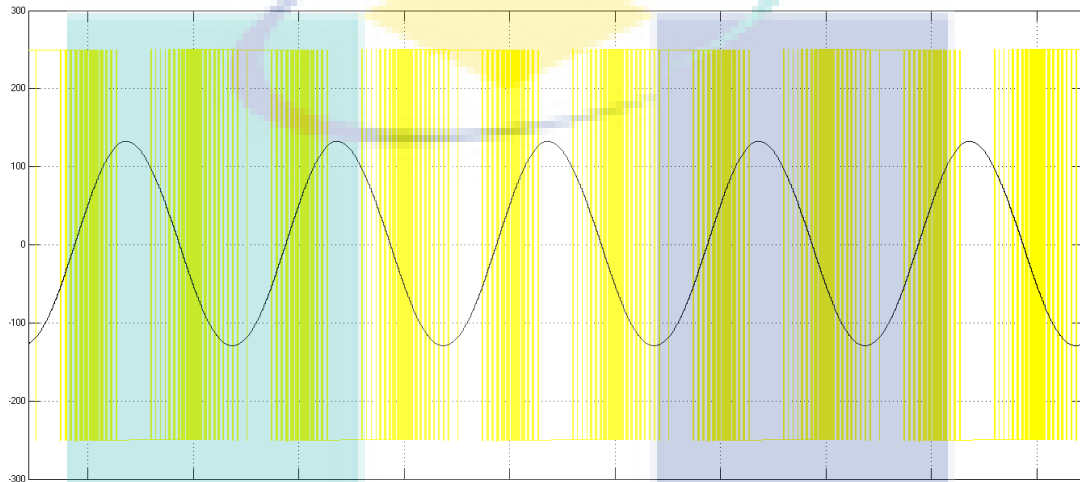


Figure 4.8 Input and output voltage of inverter,  $V_{inv}$  without current control

The same goes to output current of inverter shown in Figure 4.9, which produced total output current of  $13.2A_{rms}$ .

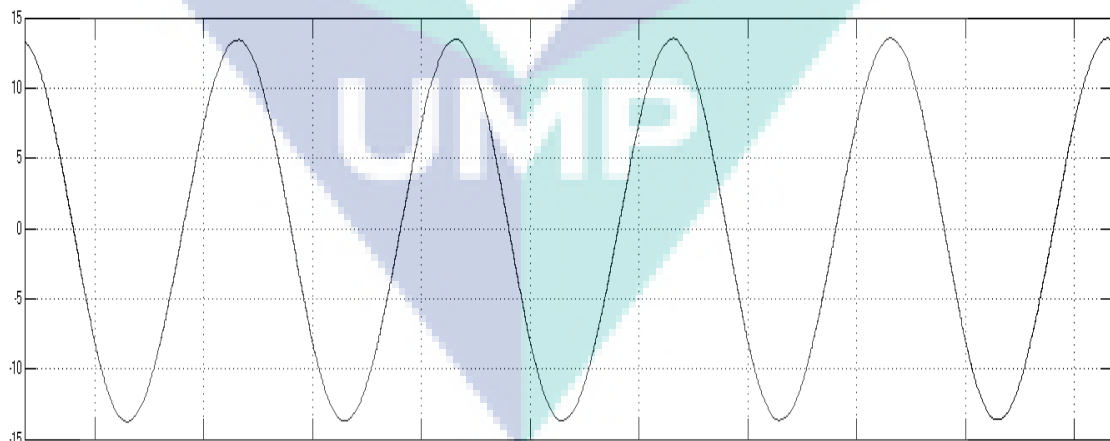


Figure 4.9 Output current inverter,  $I_{inv}$  without current control

However, the waveform quality of grid current is poor as nonlinear load draws non-sinusoidal current of  $13A_{rms}$  as demonstrated in Figure 4.10. The output signal of grid current is highly distorted without any current controllers being implemented.

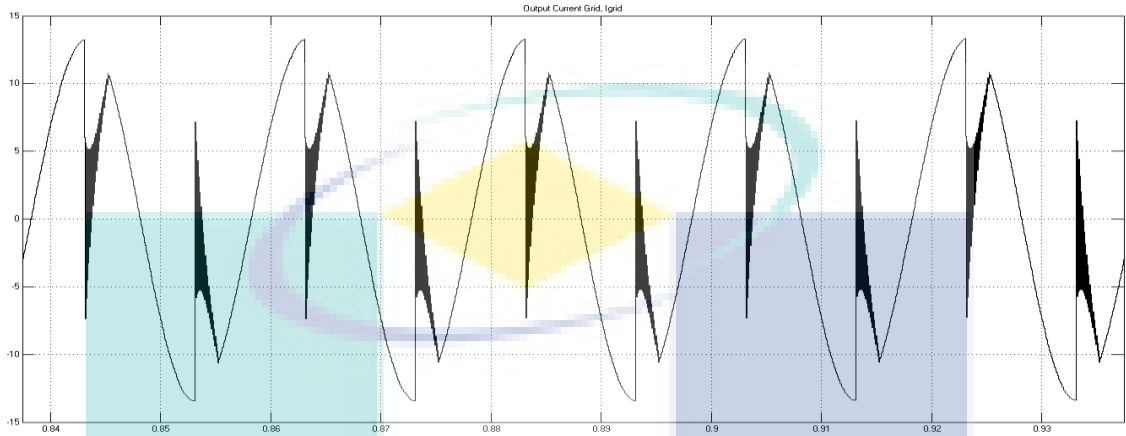


Figure 4.10 Output grid current,  $I_{grid}$  without current control

Without any current controllers, the harmonics spectrum of  $I_{grid}$  displays  $THD_i$  of 48.48% under fundamental frequency of 50Hz as shown in Figure 4.11.

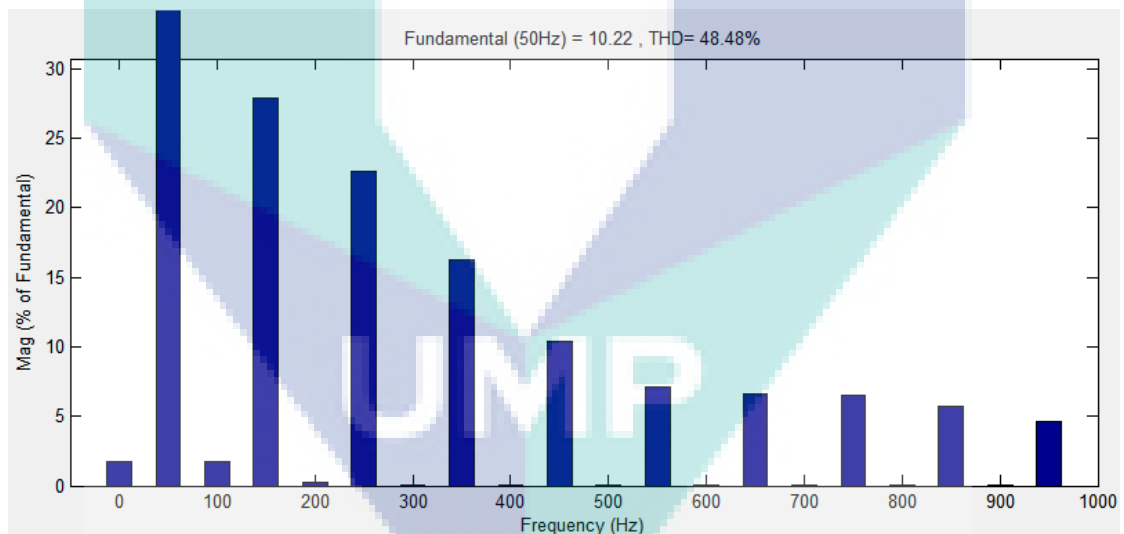


Figure 4.11  $THD_i$  of grid current,  $I_{grid}$  without current controllers



#### 4.4 Single Phase VSI Grid-Connected Inverter with Current Control

##### 4.4.1 Single Phase VSI Grid-Connected Inverter with Hysteresis Current Controller

When hysteresis current controller is added to the system, the output voltage of inverter increased from  $132.5V_{AC}$  (without current control) to  $200V_{AC}$  from the input voltage inverter of  $250V_{DC}$  as shown in Figure 4.12. As the output voltage of inverter is higher than the grid voltage, it allows power to flow from inverter to the grid system.

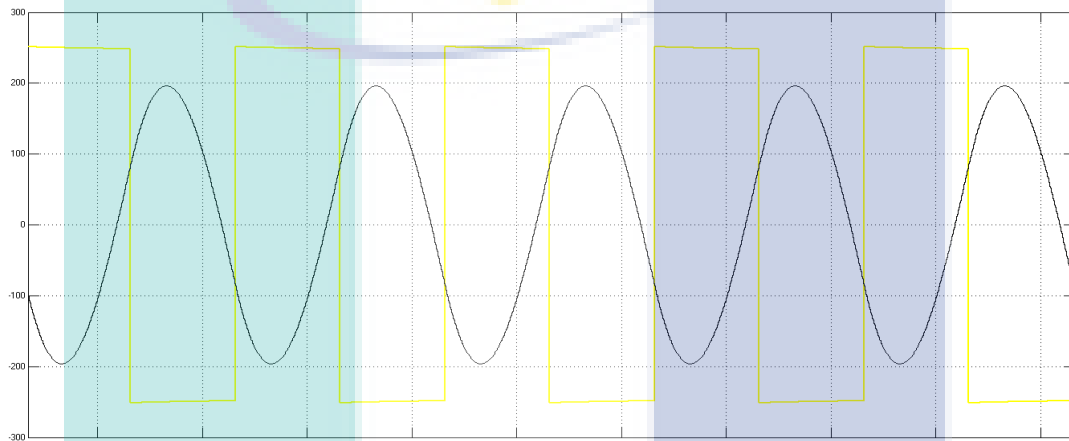


Figure 4.12 Input and output voltage inverter,  $V_{inv}$  with hysteresis current controller

The output current of inverter also increase in value, from  $13.2A_{rms}$  to  $62A_{rms}$  as shown in Figure 4.13.

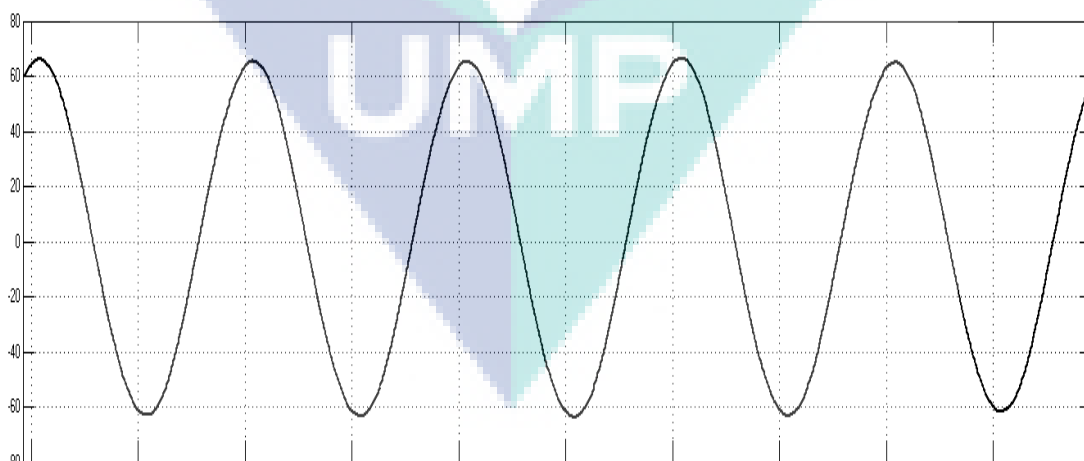


Figure 4.13 Output current inverter,  $I_{inv}$  with hysteresis current controller

As can be seen from Figure 4.14, the output grid current,  $I_{grid}$  shows better state of waveform and almost sinusoidal shape when hysteresis current controller is used to compensate the disturbance in signal. Despite of this, the waveform of grid current still has little distortion.

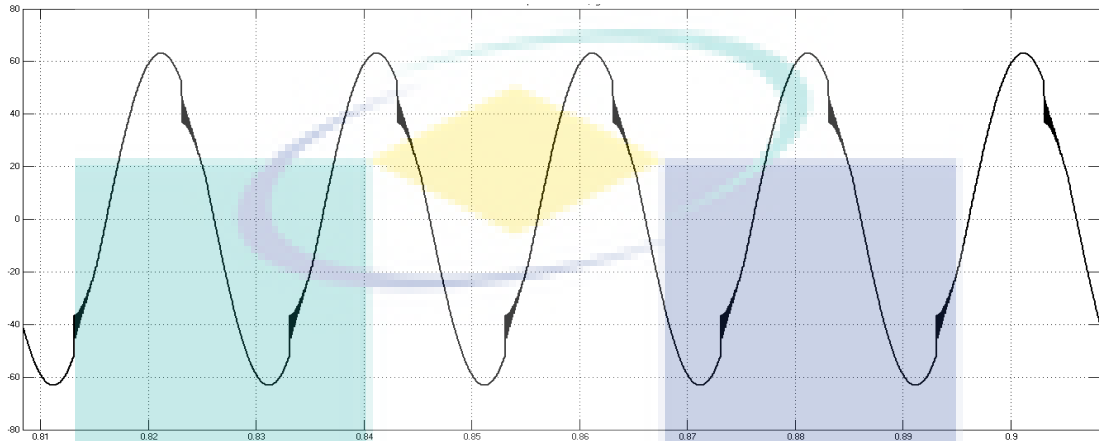


Figure 4.14 Output grid current,  $I_{grid}$  with hysteresis current controller

Hysteresis current controller exhibits a good current regulation between the inverter and grid. This can be proven from the  $THD_i$  perspective of  $I_{grid}$ , decreases from 48.48% to 5.47% shown in Figure 4.15. Although hysteresis controller shows good control performance, it is still unable to reach desired  $THD_i$  value of below 5% as recommended by IEEE 519-2014 Standard.

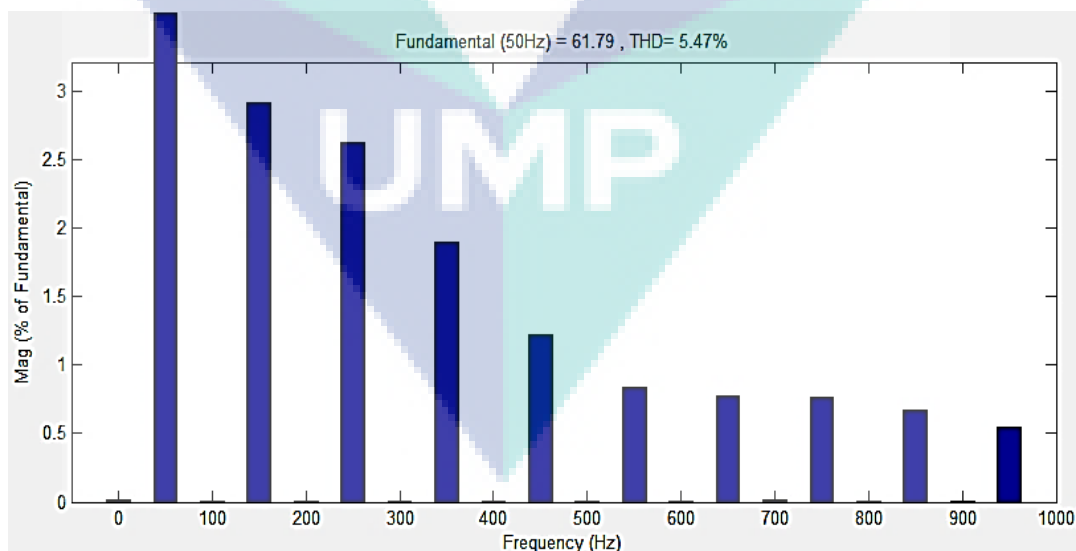


Figure 4.15  $THD_i$  of grid current,  $I_{grid}$  for hysteresis current control

#### 4.4.2 Single Phase VSI Grid-Connected Inverter with PI Controller

Referring to Figure 4.16, the output voltage of inverter is approximately  $200V_{AC}$ , with sinusoidal state waveform from  $250V_{DC}$  input voltage inverter. As mentioned earlier, power flow between inverter and grid can occur as the output voltage inverter is higher than grid voltage.

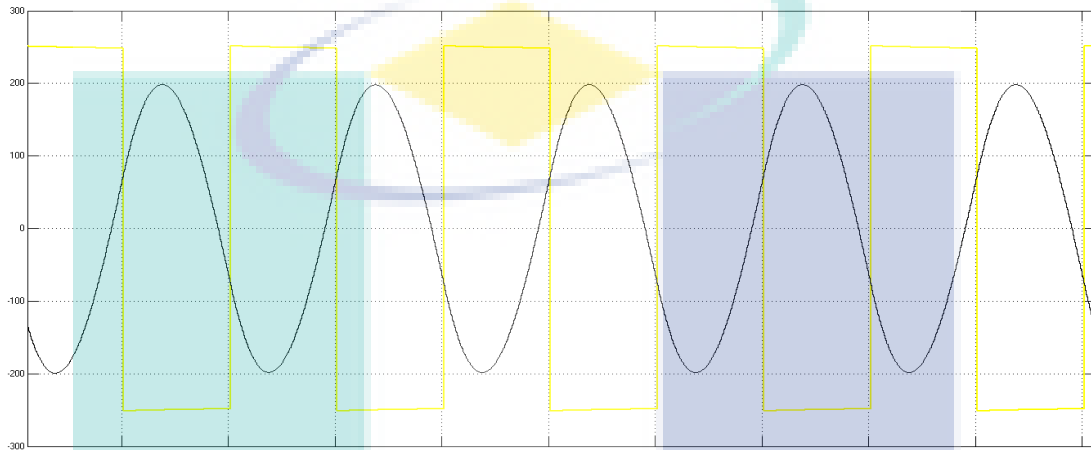


Figure 4.16 Input and output voltage inverter,  $V_{inv}$  with PI controller

For output current of inverter demonstrated in Figure 4.17, it also increases from  $13.2A_{rms}$  (without current controller) to  $65A_{rms}$  (with PI controller).

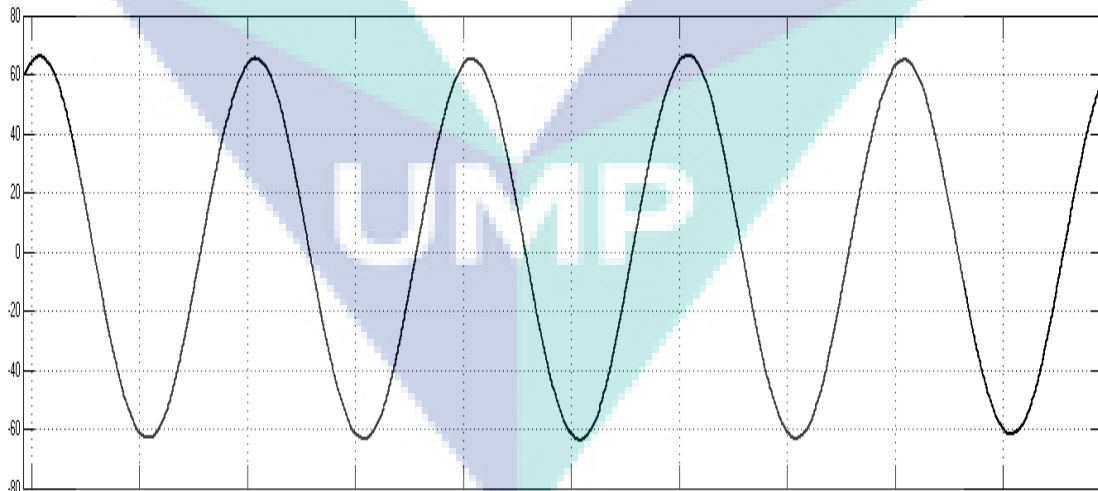


Figure 4.17 Output current inverter,  $I_{inv}$  with PI controller

As can be seen from Figure 4.18, the output grid current,  $I_{grid}$  shows better state of waveform and almost sinusoidal shape when PI controller is implemented in the system. Despite of this, the waveform of grid current still has little distortion.

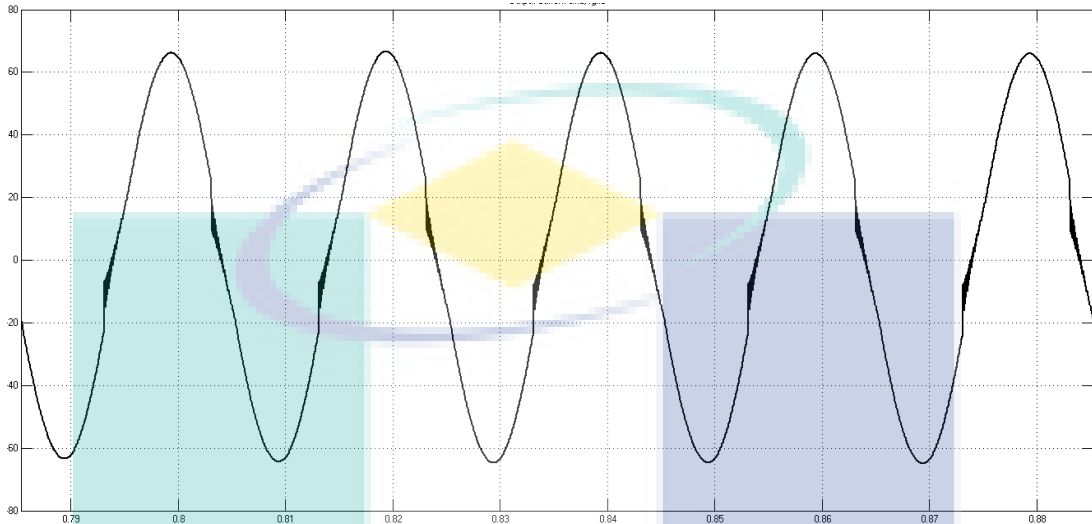


Figure 4.18 Output grid current,  $I_{grid}$  with PI controller

Unlike hysteresis current controller, PI controller exhibits a slower response of current regulation between the inverter and grid. The  $THD_i$  of  $I_{grid}$  obtained decreases from 48.48% to 5.68% as illustrated in Figure 4.19. It is still above 5% as recommended by IEEE 519-2014 Standard although the PI controller managed to reduce the distortion in grid current signal.

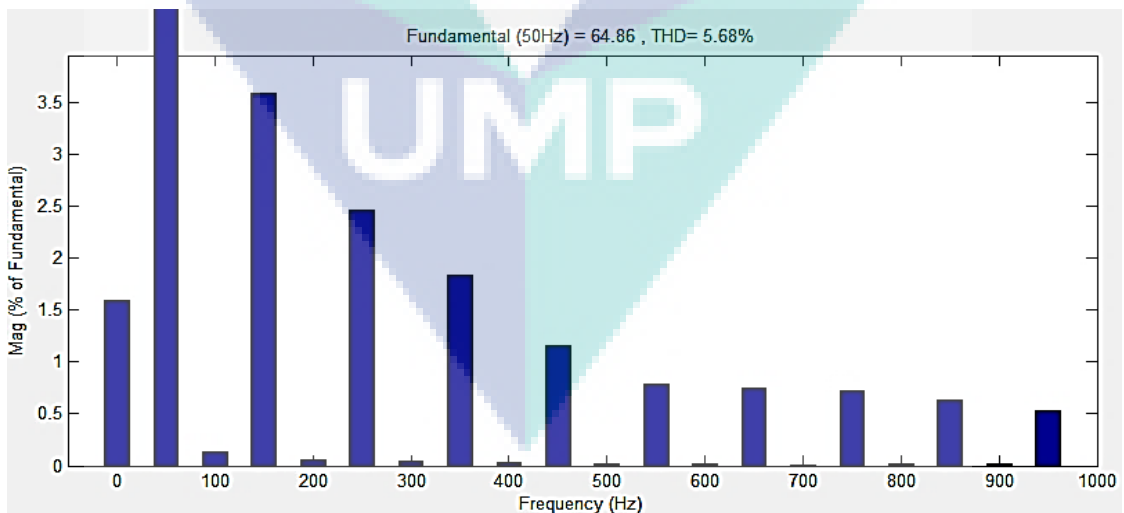


Figure 4.19  $THD_i$  of grid current,  $I_{grid}$  for PI controller

#### 4.4.3 Single Phase VSI Grid-Connected Inverter with PI with Hysteresis Current Controller

As PI controller is combined with hysteresis current controller, the output voltage of inverter is  $198V_{AC}$  from the input of  $250V_{DC}$  voltage inverter as shown in Figure 4.20. This indicates that power interchange from inverter to grid can occur.

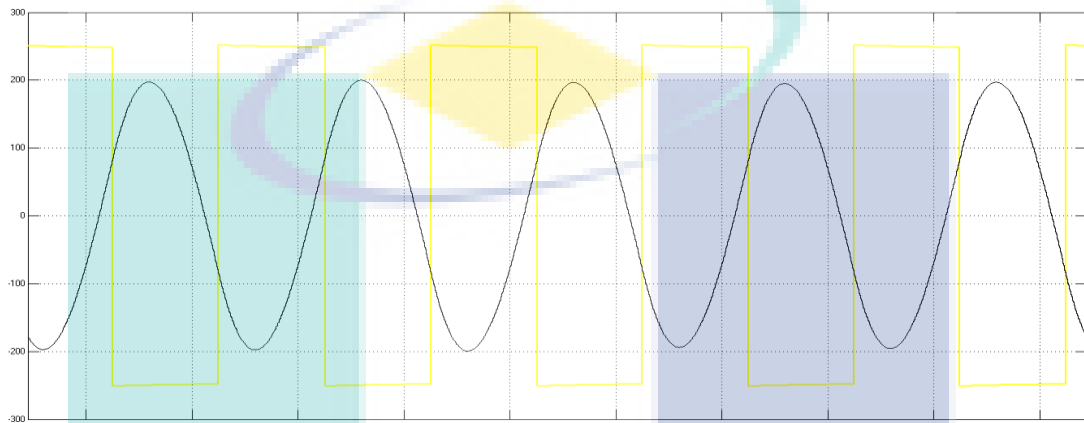


Figure 4.20 Input and output voltage inverter,  $V_{inv}$  of PI with hysteresis current controller

As the output voltage of inverter increases, the output current of inverter also shows increase in value, from  $13.2A_{rms}$  to  $66A_{rms}$  as presented in Figure 4.21.

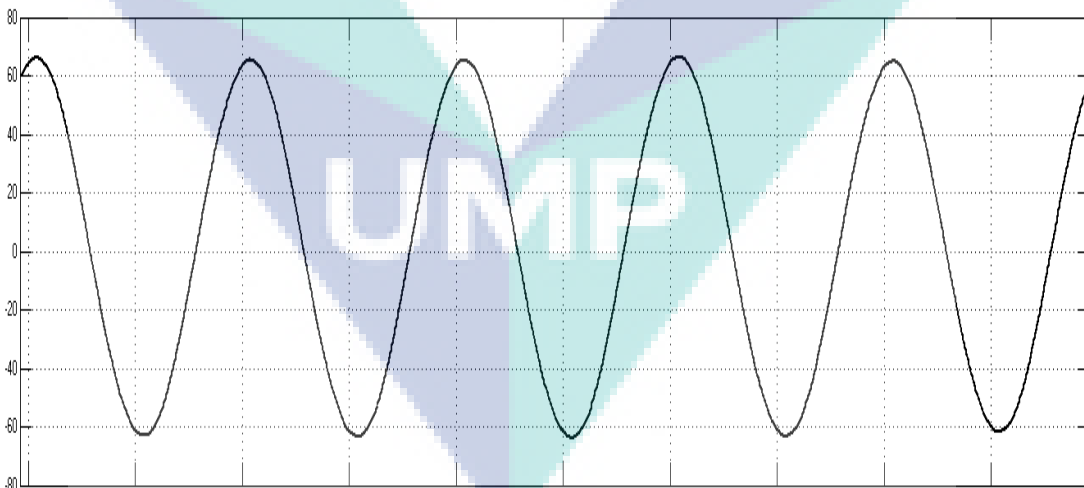


Figure 4.21 Output current inverter,  $I_{inv}$  of PI with hysteresis current controller

The output waveform of  $I_{grid}$  demonstrated in Figure 4.22 proves that the combination of both controllers (PI with hysteresis controller) managed to reduce the disturbance in signal. Although the output waveform of  $I_{grid}$  is in sinusoidal state, there is still little distortion present in the signal.

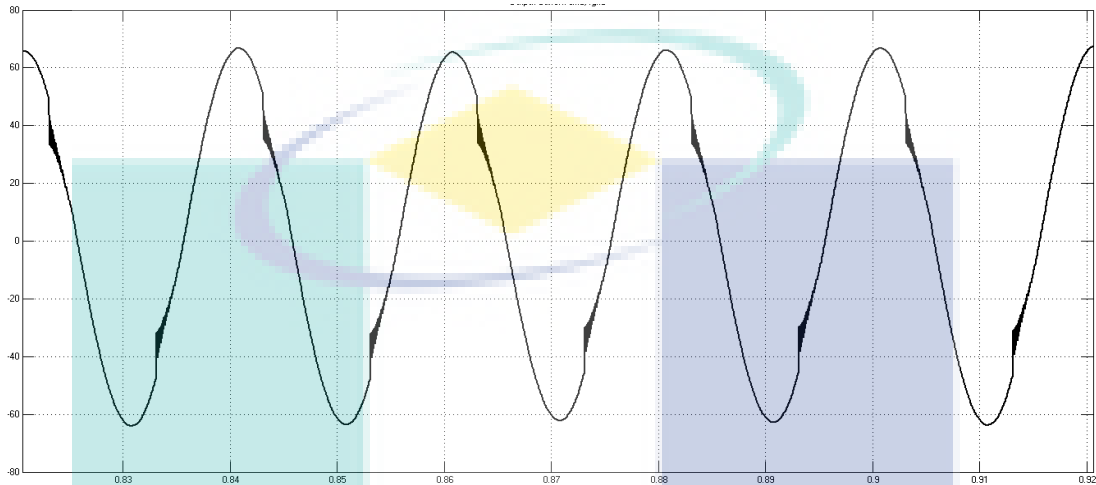


Figure 4.22 Output grid current,  $I_{grid}$  of PI with Hysteresis current controller

In this project, PI with hysteresis current controller is ranked as second best control with  $THD_i$  of grid current of 5.53% as presented in Figure 4.23. It is still higher than the desired value of achieving below 5% as preferred by IEEE 519-2014 Standard.

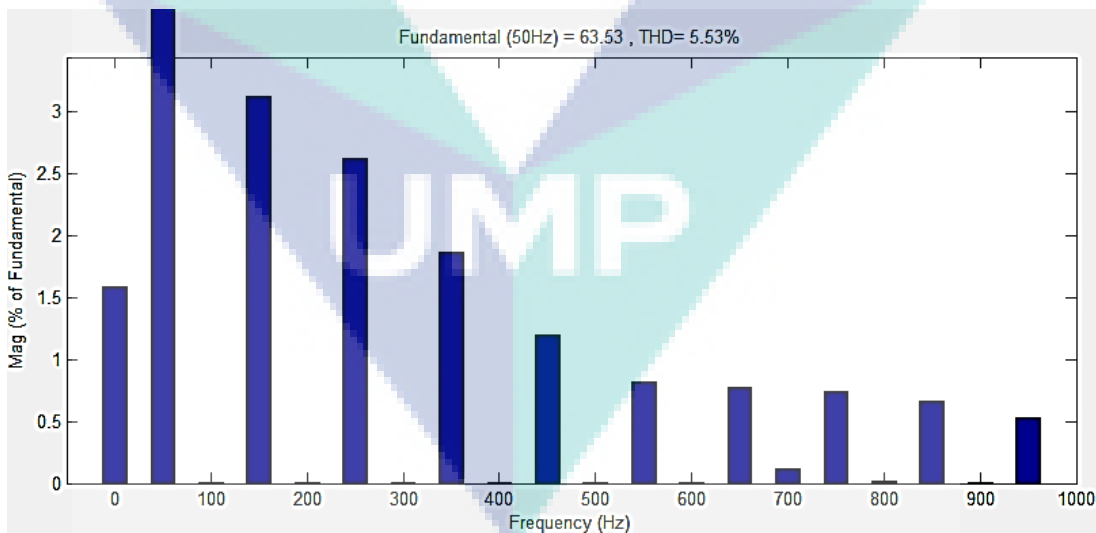
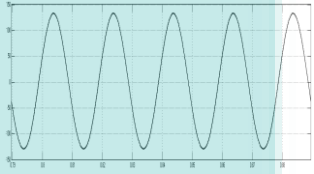
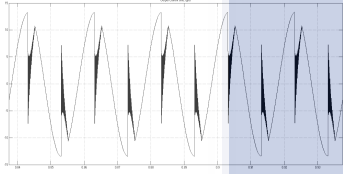
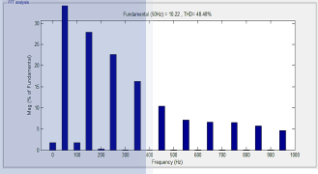

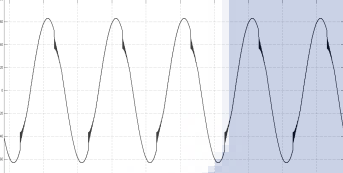
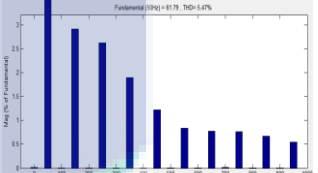
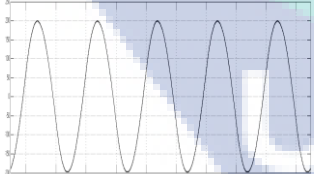
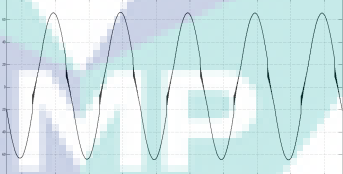
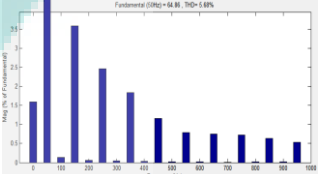
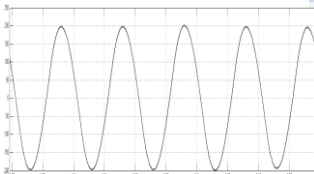
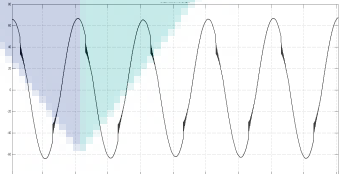
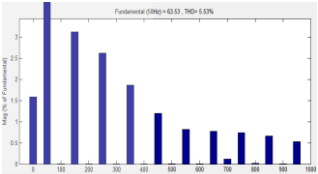


Figure 4.23  $THD_i$  of grid current,  $I_{grid}$  for PI with Hysteresis Current Controller

#### 4.5 Table of Comparison between Current Controllers

Table 4-2 summarise the overall performance of all three controllers in terms of  $V_{inv}$ ,  $I_{grid}$  and  $THD_i$  level. The output voltage of inverter,  $V_{inv}$  increases from 132.5V to the range of 198-200V after current control is added. The same goes for output grid current,  $I_{grid}$  that shows rise in value from 13A to the range of 65-66A<sub>rms</sub> with current control in the system.

Table 4-2 Comparison of  $V_{inv}$ ,  $I_{grid}$ , and  $THD_i$  of  $I_{grid}$

	$V_{inv}$	$I_{grid}$	$THD_i$ of $I_{grid}$
Without Current Control	 <p><math>V_{inv} = 132.5V_{AC}</math> (a)</p>	 <p><math>I_{grid} = 13.2A_{rms}</math> (b)</p>	 <p><math>THD_i = 48.48\%</math> (c)</p>
Hysteresis Current Control	 <p><math>V_{inv} = 200V_{AC}</math> (d)</p>	 <p><math>I_{grid} = 62A_{rms}</math> (e)</p>	 <p><math>THD_i = 5.47\%</math> (f)</p>
PI Current Control	 <p><math>V_{inv} = 200V_{AC}</math> (g)</p>	 <p><math>I_{grid} = 65A_{rms}</math> (h)</p>	 <p><math>THD_i = 5.68\%</math> (i)</p>
PI with Hysteresis Current Control	 <p><math>V_{inv} = 198V_{AC}</math> (j)</p>	 <p><math>I_{grid} = 66A_{rms}</math> (k)</p>	 <p><math>THD_i = 5.53\%</math> (l)</p>

Before current control strategies are added to the system, the output grid current,  $I_{\text{grid}}$  is highly distorted which reduces the power quality of the system. The non-sinusoidal distortion problem however managed to be overcome through the application of PI controller, hysteresis current controller and PI with hysteresis current controller. Hysteresis current controller exhibits the best result of  $\text{THD}_i$  of 5.47%, followed by 5.53% of PI with hysteresis current controller and 5.68% of PI controller.

Although hysteresis current controller have variation in switching frequency, it has fast current response which displays a good dynamic performance. PI controller unable to generate the lowest  $\text{THD}_i$  level of  $I_{\text{grid}}$  because it has several drawbacks such as slow dynamic response and non-zero steady state error. When both controllers are combined together, the system is considered to be more stable and reliable enough to mitigate any sorts of harmonic content in signals.



UMP



#### 4.5.1 Harmonics Spectrum of $I_{grid}$

Figure 4.24 shows the lower order harmonics spectrum of  $I_{grid}$  of all three current control methods. The fundamental component is excluded in order to highlight the harmonic content. Hysteresis current controller displayed the highest harmonic content from 5<sup>th</sup> order to 19<sup>th</sup> order of harmonics. This is because hysteresis current controller allows the current to flow freely within its hysteresis band, resulting in lower order harmonics. Apart from that, variation in switching frequency of hysteresis current controller also contributes to this factor.

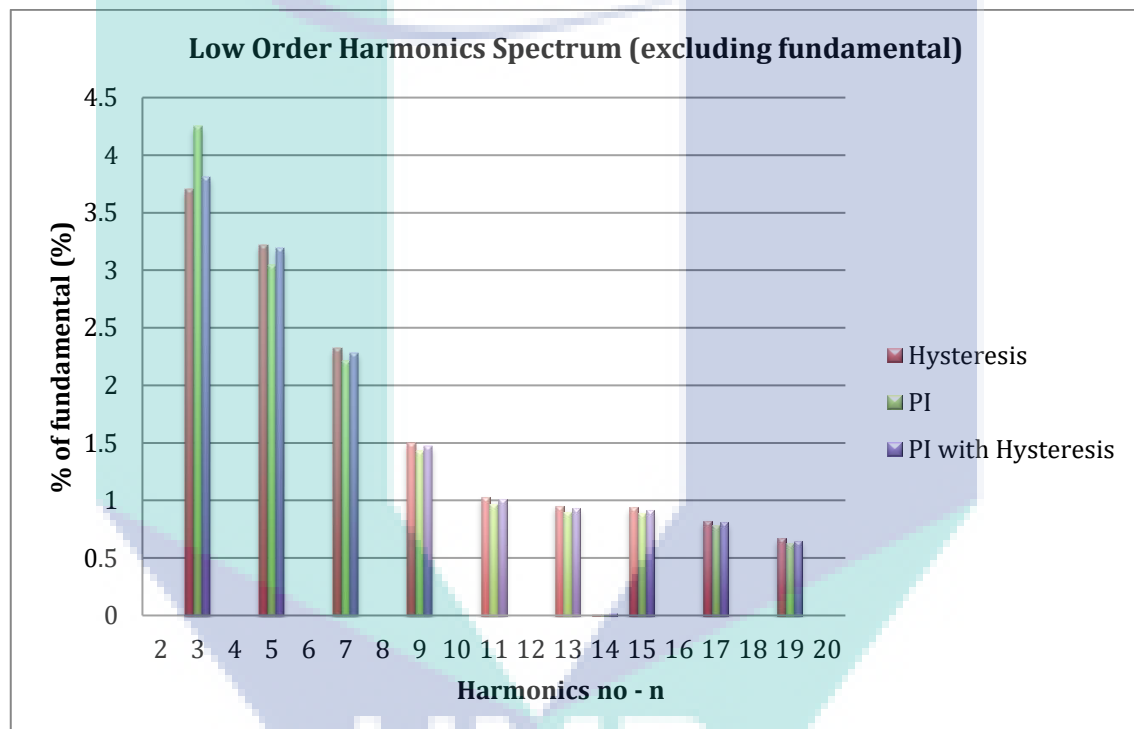


Figure 4.24 Harmonics spectrum of  $I_{grid}$  given by all three current controllers

The higher order harmonics is absent in the harmonic spectrum. This is because there are inductance being used in the circuit of project. Inductance is represented as  $R+j\omega L$ , where  $\omega$  is equal to  $2\pi f$ . The inductance is directly proportional to the frequency. When impedance is high, the order of harmonics also increases, resulting in lesser magnitude as compared to lower order harmonics. This is why filters are used to block the higher order harmonics.

#### 4.5.2 THD<sub>i</sub> Comparison of Without and With Current Controllers

Based on Figure 4.25, the distortion in  $I_{grid}$  is greatly reduced after all three current controllers are used to compensate the harmonics distortion problem. From 48.48% of THD<sub>i</sub> in  $I_{grid}$  without current controller, hysteresis current controller exhibits the lowest THD<sub>i</sub> of 5.47%. The second best current control method with THD<sub>i</sub> of 5.53% is the PI with hysteresis current controller, followed by PI controller of 5.68%.

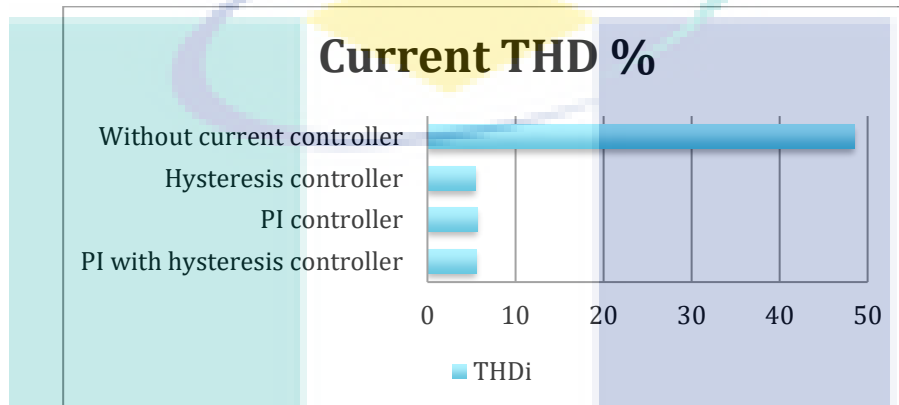


Figure 4.25 Current THD% of without and with current controllers

Table 4-3 THD<sub>i</sub> values of  $I_{grid}$  without and with current controllers

	<b>Without current controller</b>	<b>Hysteresis controller</b>	<b>PI controller</b>	<b>PI with hysteresis controller</b>
<b>THD<sub>i</sub> (%)</b>	48.48	5.47	5.68	5.53

From the THD<sub>i</sub> values obtained which are presented in Table 4-3, PI controller is observed to deliver the highest distortion due to its slow response, resulting in non-zero steady state error. Hysteresis controller shows better total harmonic distortion than PI controller due to its fast response current loop but have low order harmonics and variation in switching frequency. The combination of PI with hysteresis current controller makes the system more robust.

## CHAPTER 5

### CONCLUSION

#### 5.1 Summary of Project

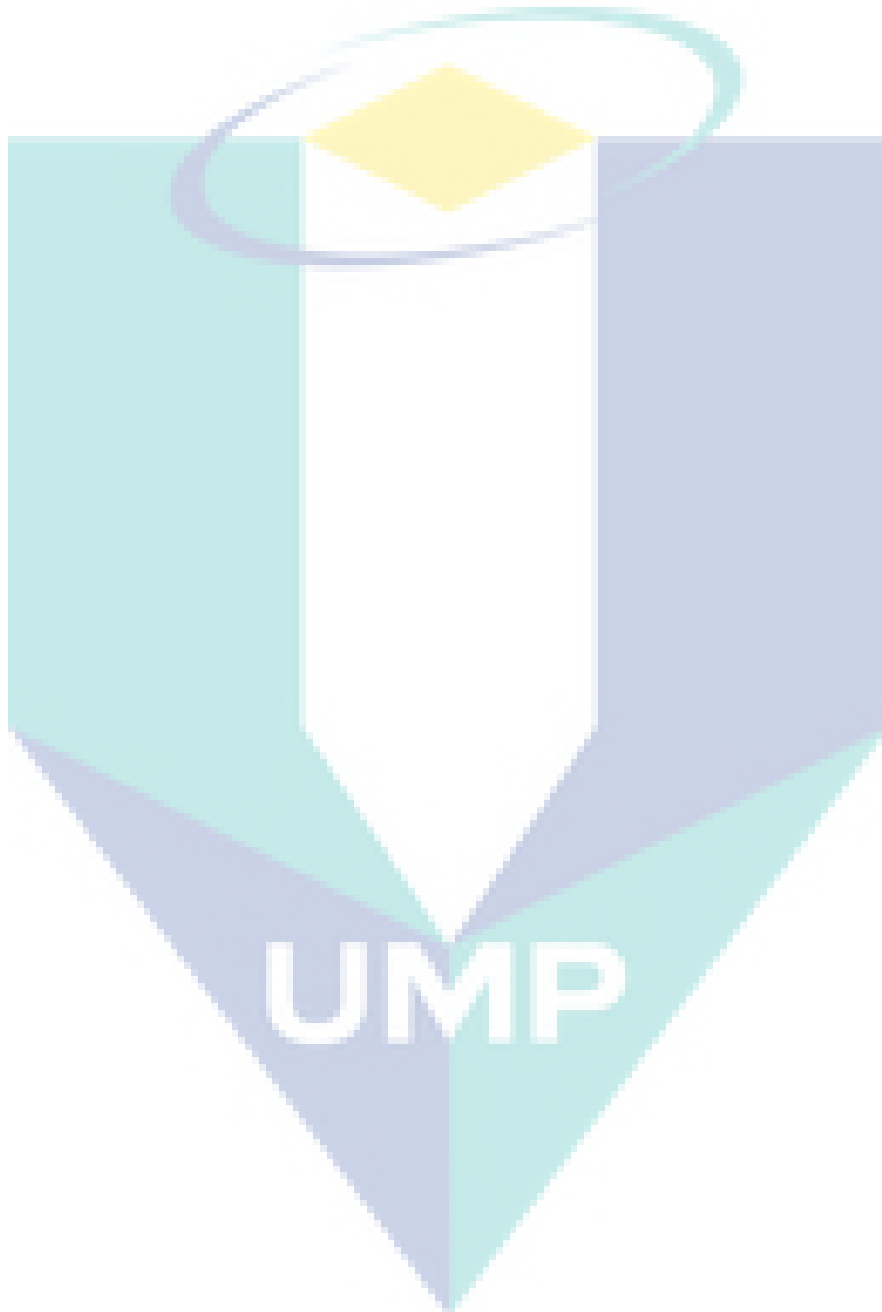
The design of single phase inverter with LC filter tested under critical load, known as nonlinear load had been developed in MATLAB<sup>TM</sup> Simulink which achieved the first target of the project. The next objective which is designing current control strategies namely hysteresis current controller, PI controller and combination of PI with hysteresis current controller had also been implemented in the single phase grid-connected inverter simulation. All of the three controllers are tested to shape the grid current as sinusoidal as possible without affecting the output voltage and current of inverter. In addition, comparative study of current controllers had also been done to accomplish the third objective, where hysteresis controller exhibits the best and fast current control response, followed by combination PI with hysteresis controller which makes the system more sturdy and PI controller as the third best due to its inability to inherit zero steady state error. In short, all of the objectives of the project are accomplished successfully.

#### 5.2 Suggestions/Recommendations for Future Work

In order to strengthen understandings theoretically and in practical on the single-phase grid-connected system and current controllers, some of the future ideas are made for further improvement of project. The recommendations are :

- i. For more precise of verification of simulation result, hardware implementation for single phase grid-connected system with current controllers namely hysteresis current controller, PI controller and combination of PI with hysteresis current controller can be suggested to observe the performance of controllers. Due to time constraint, this project is able to prove the desired results through simulation environment only.

- ii. Application of phase locked loop (PLL) method or any other grid synchronization methods in hardware system.



## REFERENCES

- [1] A. Chatterjee and K. B. Mohanty, "Current control strategies for single phase grid integrated inverters for photovoltaic applications-a review," *Renewable and Sustainable Energy Reviews*. 2018.
- [2] Z. Yao and L. Xiao, "Control of single-phase grid-connected inverters with nonlinear loads," *IEEE Trans. Ind. Electron.*, 2013.
- [3] S. Jena, B. Mohapatra, C. K. Panigrahi, and S. K. Mohanty, "Power quality improvement of 1- $\phi$  grid integrated pulse width modulated voltage source inverter using hysteresis Current Controller with offset band," in *ICACCS 2016 - 3rd International Conference on Advanced Computing and Communication Systems: Bringing to the Table, Futuristic Technologies from Around the Globe*, 2016.
- [4] S. Jena, C. K. Panigrahi, S. Sahoo, and S. K. Behera, "Current harmonics reduction of three phase grid connected pulse width modulated voltage source inverter by hysteresis current controller with offset band," in *India International Conference on Power Electronics, IICPE*, 2017.
- [5] P. A. Dahono, "New hysteresis current controller for single-phase full-bridge inverters," *IET Power Electron.*, 2009.
- [6] S. M. Cherati, N. A. Azli, S. M. Ayob, and A. Mortezaei, "Design of a current mode PI controller for a single-phase PWM inverter," in *2011 IEEE Applied Power Electronics Colloquium, IAPEC 2011*, 2011.
- [7] S. Jena, B. C. Babu, A. K. Naik, and G. Mishra, "Performance improvement of single-phase grid - Connected PWM inverter using PI with hysteresis current controller," in *Proceedings - 2011 International Conference on Energy, Automation and Signal, ICEAS - 2011*, 2011.
- [8] B.-J. Kang and C. M. Liaw, "Robust hysteresis current-controlled PWM scheme with fixed switching frequency," *IEE Proc. Electr. Power Appl.*, 2001.

- [9] A. I. Maswood and M. A. Rahman, "Performance parameters of a pulse-width modulation voltage source inverter with proportional-integral controller under non-ideal conditions," *Electr. Power Syst. Res.*, 1996.
- [10] A. Nachiappan, K. Sundararajan, and V. Malarselvam, "Current controlled voltage source inverter using hysteresis controller and PI controller," in *2012 International Conference on Power, Signals, Controls and Computation, EPSCICON 2012*, 2012.
- [11] G. M. Tina and G. Celsa, "A Matlab/Simulink model of a grid connected single-phase inverter," in *Proceedings of the Universities Power Engineering Conference*, 2015.
- [12] A. Tilli and A. Tonielli, "Sequential design of hysteresis current controller for three-phase inverter," *IEEE Trans. Ind. Electron.*, 1998.
- [13] H. Daniyal, E. Lam, L. J. Borle, and H. H. C. Iu, "Hysteresis, PI and Ramp-time Current Control Techniques for APF: An experimental comparison," in *Proceedings of the 2011 6th IEEE Conference on Industrial Electronics and Applications, ICIEA 2011*, 2011.
- [14] M. C. Trigg, "Matlab Simulink Modelling of a Single-Phase Voltage Controlled Voltage Source Inverter," *Electr. Eng.*, 2006.
- [15] B. Majhi, "Analysis of Single-Phase SPWM Inverter," *Int. J. Sci. Res.*, 2014.
- [16] A. M. Gole, "Sinusoidal Pulse width modulation," *Power Electron.*, 2000.
- [17] D. Van, "Pulse width modulation inverter.," *EP Pat. 0,273,899*, 1988.
- [18] T. C. A. Ajot, S. Salimin, and R. Aziz, "Application of PI Current Controller in Single Phase Inverter System Connected to Non Linear Load," in *IOP Conference Series: Materials Science and Engineering*, 2017.

- [19] A. I. Putri, A. Rizqiawan, F. Rozzi, N. Zakkia, Y. Haroen, and P. A. Dahono, "A hysteresis current controller for grid-connected inverter with reduced losses," in *2016 2nd International Conference of Industrial, Mechanical, Electrical, and Chemical Engineering, ICIMECE 2016*, 2017.
- [20] N. Jaalam, N. A. Rahim, A. H. A. Bakar, C. K. Tan, and A. M. A. Haidar, "A comprehensive review of synchronization methods for grid-connected converters of renewable energy source," *Renewable and Sustainable Energy Reviews*. 2016.
- [21] A. Reznik, M. G. Simoes, A. Al-Durra, and S. M. Muyeen, "LCL Filter design and performance analysis for grid-interconnected systems," *IEEE Trans. Ind. Appl.*, 2014.
- [22] C. Picardi, D. Sgrò, and G. Gioffré, "A simple and low-cost PLL structure for single-phase grid-connected inverters," in *SPEEDAM 2010 - International Symposium on Power Electronics, Electrical Drives, Automation and Motion*, 2010.
- [23] I. P. and E. Society, "IEEE Recommended Practice and Requirements for Harmonic Control in Electric Power Systems IEEE Power and Energy Society," *ANSI/IEEE Std. 519*, 2014.
- [24] C. N. M. Ho, V. S. P. Cheung, and H. S. H. Chung, "Constant-frequency hysteresis current control of grid-connected VSI without bandwidth control," *IEEE Trans. Power Electron.*, 2009.
- [25] R. P, R. I. Vais, S. Yadav, and P. Swarup, "A Modified PI Control for Grid-tied Inverters to Improve Grid Injected Current Quality," *Int. J. Eng. Technol.*, 2017.
- [26] A. Menti, T. Zacharias, and J. Miliadis-Argitis, "Harmonic distortion assessment for a single-phase grid-connected photovoltaic system," *Renew. Energy*, 2011.
- [27] K. T. Tan, P. L. So, Y. C. Chu, and M. Z. Q. Chen, "Coordinated Control and Energy Management of Distributed Generation Inverters in a Microgrid," *IEEE*

*Trans. Power Deliv.*, 2013.

- [28] K. Zeb *et al.*, “A comprehensive review on inverter topologies and control strategies for grid connected photovoltaic system,” *Renewable and Sustainable Energy Reviews*. 2018.
- [29] P. Electronics, D. L. Stra, and D. Tel, “Voltage Source Inverters for Grid Connected Photovoltaic Systems,” *Simulation*, 1998.

